

World Journal of *Clinical Cases*

World J Clin Cases 2024 February 6; 12(4): 671-871



EDITORIAL

- 671 Tenosynovitis of hand: Causes and complications
Muthu S, Annamalai S, Kandasamy V
- 677 Early antiplatelet therapy used for acute ischemic stroke and intracranial hemorrhage
Buddhavarapu V, Kashyap R, Surani S

MINIREVIEWS

- 681 Postoperative accurate pain assessment of children and artificial intelligence: A medical hypothesis and planned study
Yue JM, Wang Q, Liu B, Zhou L
- 688 Application and mechanisms of Sanhua Decoction in the treatment of cerebral ischemia-reperfusion injury
Wang YK, Lin H, Wang SR, Bian RT, Tong Y, Zhang WT, Cui YL

ORIGINAL ARTICLE**Clinical and Translational Research**

- 700 Identification and validation of a new prognostic signature based on cancer-associated fibroblast-driven genes in breast cancer
Wu ZZ, Wei YJ, Li T, Zheng J, Liu YF, Han M

Retrospective Study

- 721 Rehabilitation care for pain in elderly knee replacement patients
Liu L, Guan QZ, Wang LF
- 729 Effect of early stepwise cardiopulmonary rehabilitation on function and quality of life in sepsis patients
Zheng MH, Liu WJ, Yang J
- 737 Influence of initial check, information exchange, final accuracy check, reaction information nursing on the psychology of elderly with lung cancer
Jiang C, Ma J, He W, Zhang HY
- 746 Experience of primary intestinal lymphangiectasia in adults: Twelve case series from a tertiary referral hospital
Na JE, Kim JE, Park S, Kim ER, Hong SN, Kim YH, Chang DK

Observational Study

- 758 Perceived stress among staff in Saudi Arabian dental colleges before and after an accreditation process: A cross-sectional study
Shaiban AS

META-ANALYSIS

- 766 Comprehensive effects of traditional Chinese medicine treatment on heart failure and changes in B-type natriuretic peptide levels: A meta-analysis
Xia LL, Yang SY, Xu JY, Chen HQ, Fang ZY

CASE REPORT

- 777 Mechanical upper bowel obstruction caused by a large trichobezoar in a young woman: A very unusual case report
Scherrer M, Kornprat P, Sucher R, Muehlsteiner J, Wagner D
- 782 Accidental placement of venous return catheter in the superior vena cava during venovenous extracorporeal membrane oxygenation for severe pneumonia: A case report
Song XQ, Jiang YL, Zou XB, Chen SC, Qu AJ, Guo LL
- 787 Gestational diabetes mellitus combined with fulminant type 1 diabetes mellitus, four cases of double diabetes: A case report
Li H, Chai Y, Guo WH, Huang YM, Zhang XN, Feng WL, He Q, Cui J, Liu M
- 795 Clinical experience sharing on gastric microneuroendocrine tumors: A case report
Wang YJ, Fan DM, Xu YS, Zhao Q, Li ZF
- 801 Endoscopic retrograde appendicitis treatment for periappendiceal abscess: A case report
Li QM, Ye B, Liu JW, Yang SW
- 806 Hemichorea in patients with temporal lobe infarcts: Two case reports
Wang XD, Li X, Pan CL
- 814 Monomorphic epitheliotropic intestinal T-cell lymphoma with bone marrow involved: A case report
Zhang FJ, Fang WJ, Zhang CJ
- 820 Inetetamab combined with tegafur as second-line treatment for human epidermal growth factor receptor-2-positive gastric cancer: A case report
Zhou JH, Yi QJ, Li MY, Xu Y, Dong Q, Wang CY, Liu HY
- 828 Pedicled abdominal flap using deep inferior epigastric artery perforators for forearm reconstruction: A case report
Jeon JH, Kim KW, Jeon HB
- 835 Individualized anti-thrombotic therapy for acute myocardial infarction complicated with left ventricular thrombus: A case report
Song Y, Li H, Zhang X, Wang L, Xu HY, Lu ZC, Wang XG, Liu B
- 842 Multiple paradoxical embolisms caused by central venous catheter thrombus passing through a patent foramen ovale: A case report
Li JD, Xu N, Zhao Q, Li B, Li L

- 847** Rupture of a giant jejunal mesenteric cystic lymphangioma misdiagnosed as ovarian torsion: A case report
Xu J, Lv TF
- 853** Adenocarcinoma of sigmoid colon with metastasis to an ovarian mature teratoma: A case report
Wang W, Lin CC, Liang WY, Chang SC, Jiang JK
- 859** Perforated gastric ulcer causing mediastinal emphysema: A case report
Dai ZC, Gui XW, Yang FH, Zhang HY, Zhang WF
- 865** Appendicitis combined with Meckel's diverticulum obstruction, perforation, and inflammation in children: Three case reports
Sun YM, Xin W, Liu YF, Guan ZM, Du HW, Sun NN, Liu YD

ABOUT COVER

Peer Reviewer of *World Journal of Clinical Cases*, Che-Chun Su, MD, PhD, Associate Professor, Department of Internal Medicine, Changhua Christian Hospital, Changhua 500, Taiwan. 115025@cch.org.tw

AIMS AND SCOPE

The primary aim of *World Journal of Clinical Cases* (*WJCC*, *World J Clin Cases*) is to provide scholars and readers from various fields of clinical medicine with a platform to publish high-quality clinical research articles and communicate their research findings online.

WJCC mainly publishes articles reporting research results and findings obtained in the field of clinical medicine and covering a wide range of topics, including case control studies, retrospective cohort studies, retrospective studies, clinical trials studies, observational studies, prospective studies, randomized controlled trials, randomized clinical trials, systematic reviews, meta-analysis, and case reports.

INDEXING/ABSTRACTING

The *WJCC* is now abstracted and indexed in Science Citation Index Expanded (SCIE, also known as SciSearch®), Journal Citation Reports/Science Edition, Current Contents®/Clinical Medicine, PubMed, PubMed Central, Reference Citation Analysis, China Science and Technology Journal Database, and Superstar Journals Database. The 2023 Edition of Journal Citation Reports® cites the 2022 impact factor (IF) for *WJCC* as 1.1; IF without journal self cites: 1.1; 5-year IF: 1.3; Journal Citation Indicator: 0.26; Ranking: 133 among 167 journals in medicine, general and internal; and Quartile category: Q4.

RESPONSIBLE EDITORS FOR THIS ISSUE

Production Editor: *Si Zhao*; Production Department Director: *Xu Guo*; Editorial Office Director: *Jin-Lai Wang*.

NAME OF JOURNAL

World Journal of Clinical Cases

ISSN

ISSN 2307-8960 (online)

LAUNCH DATE

April 16, 2013

FREQUENCY

Thrice Monthly

EDITORS-IN-CHIEF

Bao-Gan Peng, Salim Surani, Jerzy Tadeusz Chudek, George Kontogeorgos, Maurizio Serati

POLICY OF CO-AUTHORS**EDITORIAL BOARD MEMBERS**

<https://www.wjgnet.com/2307-8960/editorialboard.htm>

PUBLICATION DATE

February 6, 2024

COPYRIGHT

© 2024 Baishideng Publishing Group Inc

INSTRUCTIONS TO AUTHORS

<https://www.wjgnet.com/bpg/gerinfo/204>

GUIDELINES FOR ETHICS DOCUMENTS

<https://www.wjgnet.com/bpg/GerInfo/287>

GUIDELINES FOR NON-NATIVE SPEAKERS OF ENGLISH

<https://www.wjgnet.com/bpg/gerinfo/240>

PUBLICATION ETHICS

<https://www.wjgnet.com/bpg/GerInfo/288>

PUBLICATION MISCONDUCT

<https://www.wjgnet.com/bpg/gerinfo/208>

<https://www.wjgnet.com/bpg/GerInfo/310>

ARTICLE PROCESSING CHARGE

<https://www.wjgnet.com/bpg/gerinfo/242>

STEPS FOR SUBMITTING MANUSCRIPTS

<https://www.wjgnet.com/bpg/GerInfo/239>

ONLINE SUBMISSION

<https://www.f6publishing.com>



Clinical and Translational Research

Identification and validation of a new prognostic signature based on cancer-associated fibroblast-driven genes in breast cancer

Zi-Zheng Wu, Yuan-Jun Wei, Tong Li, Jie Zheng, Yin-Feng Liu, Meng Han

Specialty type: Oncology

Provenance and peer review:

Unsolicited article; Externally peer reviewed.

Peer-review model: Single blind

Peer-review report's scientific quality classification

Grade A (Excellent): 0

Grade B (Very good): 0

Grade C (Good): C, C, C

Grade D (Fair): 0

Grade E (Poor): 0

P-Reviewer: Bansal C, India;
Papadopoulos VP, Greece

Received: December 1, 2023

Peer-review started: December 1, 2023

First decision: December 7, 2023

Revised: December 14, 2023

Accepted: January 3, 2024

Article in press: January 3, 2024

Published online: February 6, 2024



Zi-Zheng Wu, Yuan-Jun Wei, Tong Li, Jie Zheng, Yin-Feng Liu, Meng Han, Breast Disease Diagnosis and Treatment Center, The First Hospital of Qinhuangdao, Qinhuangdao 066000, Hebei Province, China

Yuan-Jun Wei, Meng Han, Department of General Surgery, Hebei Medical University, Shijiazhuang 050000, Hebei Province, China

Yuan-Jun Wei, Meng Han, Breast Disease Diagnosis and Treatment Center, The First Hospital of Qinhuangdao, Hebei Medical University, Qinhuangdao 066000, Hebei Province, China

Tong Li, Breast Disease Diagnosis and Treatment Center, Chengde Medical College, Chengde 067000, Hebei Province, China

Corresponding author: Meng Han, MD, Director, Breast Disease Diagnosis and Treatment Center, The First Hospital of Qinhuangdao, No. 258 Wenhua Road, Haigang District, Qinhuangdao 066000, Hebei Province, China. menghan68527@163.com

Abstract

BACKGROUND

Breast cancer (BC), a leading malignant disease, affects women all over the world. Cancer associated fibroblasts (CAFs) stimulate epithelial-mesenchymal transition, and induce chemoresistance and immunosuppression.

AIM

To establish a CAFs-associated prognostic signature to improve BC patient outcome estimation.

METHODS

We retrieved the transcript profile and clinical data of 1072 BC samples from The Cancer Genome Atlas (TCGA) databases, and 3661 BC samples from the The Gene Expression Omnibus. CAFs and immune cell infiltrations were quantified using CIBERSORT algorithm. CAF-associated gene identification was done by weighted gene co-expression network analysis. A CAF risk signature was established *via* univariate, least absolute shrinkage and selection operator regression, and multivariate Cox regression analyses. The receiver operating characteristic (ROC) and Kaplan-Meier curves were employed to evaluate the predictability of the model. Subsequently, a nomogram was developed with the risk score and patient clinical signature. Using Spearman's correlations analysis, the relationship between CAF

risk score and gene set enrichment scores were examined. Patient samples were collected to validate gene expression by quantitative real-time polymerase chain reaction (qRT-PCR).

RESULTS

Employing an 8-gene (IL18, MYD88, GLIPR1, TNN, BHLHE41, DNAJB5, FKBP14, and XG) signature, we attempted to estimate BC patient prognosis. Based on our analysis, high-risk patients exhibited worse outcomes than low-risk patients. Multivariate analysis revealed the risk score as an independent indicator of BC patient prognosis. ROC analysis exhibited satisfactory nomogram predictability. The area under the curve showed 0.805 at 3 years, and 0.801 at 5 years in the TCGA cohort. We also demonstrated that a reduced CAF risk score was strongly associated with enhanced chemotherapeutic outcomes. CAF risk score was significantly correlated with most hallmark gene sets. Finally, the prognostic signature were further validated by qRT-PCR.

CONCLUSION

We introduced a newly-discovered CAFs-associated gene signature, which can be employed to estimate BC patient outcomes conveniently and accurately.

Key Words: Breast cancer; Prognosis; Gene signature; The Cancer Genome Atlas; The Gene Expression Omnibus

©The Author(s) 2024. Published by Baishideng Publishing Group Inc. All rights reserved.

Core Tip: Breast cancer (BC), a leading malignant disease, affects women all over the world. Cancer associated fibroblasts (CAFs) stimulate epithelial-mesenchymal transition, and induce chemoresistance and immunosuppression. We introduced a newly-discovered CAFs-associated gene signature using IL18, MYD88, GLIPR1, TNN, BHLHE41, DNAJB5, FKBP14, and XG, which can be employed to estimate BC patient outcomes conveniently and accurately.

Citation: Wu ZZ, Wei YJ, Li T, Zheng J, Liu YF, Han M. Identification and validation of a new prognostic signature based on cancer-associated fibroblast-driven genes in breast cancer. *World J Clin Cases* 2024; 12(4): 700-720

URL: <https://www.wjgnet.com/2307-8960/full/v12/i4/700.htm>

DOI: <https://dx.doi.org/10.12998/wjcc.v12.i4.700>

INTRODUCTION

Breast cancer (BC) is responsible for the most cancer-related deaths in women all over the world[1]. The Prediction Analysis of Microarray 50 (PAM50) classifies BC into five categories, namely, luminal A, luminal B, Her2-enriched, normal-like, and basal-like BC[2]. Despite this, patients with the same molecular and clinical signatures can exhibit vastly different outcomes as well as responses to chemotherapy and immunotherapy[3], suggesting the presence of unknown mediators that influence both the cancer prognosis and therapeutic response. Classical assessments such as those involving tumor-node-metastasis (TNM) staging and pathology are subjective at best and are poor at predicting patient outcomes and therapeutic responses. Hence, it is critical to develop novel approaches that are able to accurately estimate BC patient overall survival (OS) and thus improve outcomes.

Tumor pathogenesis and progression are modulated by both the cancer cells themselves and the tumor microenvironment (TME)[4]. The tumor stroma plays a critical role in enhancing tumor aggressiveness by modulating the deposition of the extracellular matrix (ECM) as well as cellular metabolism[5]. Of all TME stromal cells, cancer-associated fibroblasts (CAFs) have been the most widely examined. CAFs make up a majority of the stroma and are essential for tumor invasion, angiogenesis, and ECM remodeling, promoting cell-cell associations and the release of pro-invasive factors[6-8]. STAT3 induces breast cancer growth *via* ANGPTL4, MMP13 and STC1 secretion by cancer associated fibroblasts[9]. Cancer-associated fibroblasts facilitate premetastatic niche formation through lncRNA SNHG5-mediated angiogenesis and vascular permeability in breast cancer[10]. High expression of TGF- α , PKMYT1 and decreased SFRP1 and SFRP2 in the fibroblasts were associated with disease recurrence, invasive disease or decreased survival[11]. Hence, it is critical to explore the physiological properties of CAFs and their potential as therapeutic targets in BC.

Weighted gene co-expression network analysis (WGCNA) is an extensive bioinformatics algorithm that incorporates highly expressed genes and their associates into several gene modules to examine their association with the phenotype of interest[12]. In the past, WGCNA was successfully applied to identify CAF indicators[13,14]. To date, there have been no reports on WGCNA-based analysis of CAFs and stromal invasion in BC. Here, we reported that a CAF subtype functions as an indicator of BC patient prognosis, and we identified CAF-associated genes with prognostic significance. We also report an eight-gene signature using CAF-associated genes that can accurately estimate both OS and therapeutic response in BC patients. Our findings may highlight a novel and robust prognostic indicator for the personalized therapy of BC patients.

MATERIALS AND METHODS

Data sources and preprocessing

RNA-seq data [$\log_2(\text{FPKM}+1)$], mutation annotation format file, and corresponding clinical information of 1072 breast invasive carcinoma patients in the The Cancer Genome Atlas (TCGA) database were obtained using Xena (<https://xenabrowser.net>). The Ensemble Gene was transformed into gene symbols to retrieve transcripts *via* the annotation file (hg38, gencode.v22.annotation.gene.probemmap) of the GENCODE database[15]. Overall, 1072 primary BC samples and 99 adjoining healthy breast tissues were obtained from the TCGA. Table 1 summarizes in detail the clinical data of these primary BC patients. OS is defined as the time from diagnosis to death from any cause.

OS information was available for 1050 patients. The GSE96058, GSE18728, and GSE21653 datasets were downloaded from the The Gene Expression Omnibus (GEO) database (www.ncbi.nlm.nih.gov/geo). The GSE96058 and GSE21653 datasets served as the validation cohorts.

The CAF-related gene expression signature (reference genomes) was downloaded from previous literature. This clearly separated CAFs into five subtypes[16]. Only the gene expression values greater than 1 were included. Supplementary Table 1 lists the CAF-related expression signature.

Calculation of CAF and microenvironment cell abundance

The Cell Type Identification by Estimating Relative Subsets of Known RNA Transcripts (CIBERSORT) algorithm was employed for the enrichment estimation of the five CAF and immune cell types for BC and normal samples from the TCGA dataset[17]. The ESTIMATE algorithm computed the BC patient stromal and immune scores using the bulk gene expression data[18]. Kruskal-Wallis tests were used to compare differences in CAF and immune cell proportions, as well as stromal and immune scores in different cancer stages and normal tissues.

Using univariate analysis, we assessed the association between the five CAF phenotypes and OS. The correlations between prognostic CAF subtype, stromal and immune scores were computed *via* Pearson's correlation coefficients.

Construction of a weighted gene co-expression network and identification of CAF-associated genes

The WGCNA package was employed to construct the weighted gene co-expression network (WGCN)[12] in R software, based on mRNA expression profiling. Hierarchical clustering was used to obtain modules, with each module harboring a minimum of 30 genes (min Module Size = 30). We computed the eigengenes, clustered the modules based on hierarchy, and combined comparable modules (abline = 0.25). Pearson's correlation coefficients were calculated to assess the relationship between the modules and patient clinical signatures. The gene significance (GS) was described as the \log_{10} transformation of the matched P value ($GS = \lg P$) of the association between the gene levels and matched clinical data. To further evaluate this module, the module eigengenes (ME) dissimilarity was computed *via* the module Eigengenes function in the R WGCNA package. This was described as the primary portion of a given module and was deemed as the gene expression signature representative in a module. The module membership (MM) gene values in modules were computed by evaluating associations between gene signatures and MEs. Hub genes were chosen for $MM > \text{one-third}$ difference between the maximum and minimum MM, and $GS > \text{one-third}$ difference between the maximum and minimum GS.

Functional enrichment analysis

Gene ontology (GO), including cellular component, biological process, and molecular function (MF), and Kyoto Encyclopedia of Genes and Genomes (KEGG) network enrichment analyses were conducted on CAF-related gene hub genes and was visualized using the clusterProfile package[19] in the R software. Adjusted $P < 0.05$ was set as the significance threshold.

Construction and verification of a CAF-related gene prognostic signature CAF-related in PDF format

To build a prognosis-related signature, univariate analysis was employed to screen for OS-associated genes with P values < 0.05 . Subsequently, the marked prognostic genes underwent filtration using least absolute shrinkage and selection operator (LASSO)-penalized Cox regression analysis. Only genes with nonzero coefficients in the LASSO model were selected for additional multivariate analysis. Next, the prognostic risk model was generated based on the following: Risk score (RS, CAFPS) = $\beta \text{ gene1} \times \text{expr gene1} + \beta \text{ gene2} \times \text{expr gene2} + \dots + \beta \text{ gene n} \times \text{expr gene n}$. In this formula, β represented the correlation coefficient in multivariate analysis, and expr represented mRNA expression. The patients were then separated into a high- (HR) or low-risk (LR) cohort, based on the median RS. The same formula was employed for the RSs calculation in the GEO and TCGA datasets.

The Kaplan-Meier log-rank test and the time-dependent receiver operating characteristic (ROC) curve analysis were employed to confirm the eight-gene signature performance. The RS distribution and OS status scatter plots, as well as the expression heatmaps of the eight CAF-related risk genes between the HR and LR cohorts, were constructed to assess the prognostic signature, and the stand-alone prognostic analysis was performed to assess the independent nature of the signature in predicting OS.

Development of nomogram

To translate the prognostic significance of the eight-gene signature into clinical application, we established a nomogram involving the RS and matched clinical data of BC patients, which included age and pathological stage. In addition, the calibration curves were generated to evaluate the agreement between the true and estimated OS.

Estimation of patient therapeutic response, according to the 8-gene signature

To further confirm the predictability of CAFPS in estimating patient chemotherapeutic response, GSE18728 was employed. Differences in CAFPS between responder and non-responder cohorts were assessed *via* the Wilcoxon test.

Enrichment analyses

Furthermore, the “h.all.v7.4. symbols” gene sets were derived from the Molecular Signatures Database (MSigDB)[20]. The ssGSEA was employed to compute the hallmark gene set enrichment scores[21]. Spearman correlation analysis was used to assess the relationships between the CAFPS and gene set enrichment scores.

Patients and tissue samples

All 80 breast cancer tissues and paired adjacent normal tissues were obtained from patients treated at the first hospital of qinhuangdao between January 2022 and December 2022. The paired adjacent normal tissues were dissected by the surgeons 5-cm away from the tumor edge. Tissue samples were stored at liquid nitrogen until total RNA was extracted. This study was approved by the Ethics Committee of the first hospital of qinhuangdao, and the informed consent forms were obtained from all the patients.

Quantitative real-time polymerase chain reaction

Total RNA was isolated from the BC and matched adjacent tissues using TRIzol (Thermo Fisher Scientific). The Nanodrop 2000 (Thermo Fisher Scientific) was used to detect the purity and concentration of the total RNA. According to the manufacturer's protocol, quantitative real-time polymerase chain reaction (qRT-PCR) was performed by using Taq Pro universal SYBR qPCR Master Mix (Vazyme, Nanjing, China). The primers used were as follows: FKBP14 forward primer 5'-AGCTGATCAACATCGGCAAT-3' and reverse primer 5'- CCAAGAACCCCCATTATGA -3', β actin forward primer 5'CATGTACGTTGCTATCCAGGC3' and reverse primer 5'CTCCTAATGTACAGCAGCAT-3'. The relative levels of FKBP14 was evaluated by the $2^{-\Delta\Delta CT}$ method using β actin as the control.

Statistical analysis

All data analyses were performed in R version 3.6.4 (<https://www.r-project.org>) and associated packages. The Wilcoxon test was used to examine the CAFPS-clinicopathological properties link. Kaplan-Meier curves and log-rank tests were used for evaluating OS using the survival and survminer R packages.

RESULTS

Clinical significance of the CAF proportion in BC

The proportions of five CAF and immune cell types in BC and normal samples from the TCGA database were obtained using the CIBERSORT algorithm. We observed marked differences in the proportions of the five types of CAFs (Figure 1), CD4 memory resting T cells, CD4 memory activated T cells, regulatory T cells, resting natural killer (NK) cells, and the stromal score between different cancer stages and normal tissues (Supplementary Figure 1). Based on the median value of the CAF proportion, patients were divided into high and low CAF groups. The prognosis of patients in different groups was compared (Figure 2A-F). Patients with lower proportions of the CAF S3 subset were found to have better OS ($P = 0.015$; Figure 2D). Figure 2G and H illustrates a positive correlation between the CAF-S3 proportion and the immune ($r = 0.57$, $P < 2.2e-16$) and stromal scores ($r = 0.33$, $P < 2.2e-16$).

Use of WGCNA to develop a principal-gene module related to CAF-S3 cells

To better represent the scale-free topology of the co-expression axis in the WGCNA, we chose the soft-threshold $\beta = 6$ (Figure 3A). Ten co-expressed gene modules were clustered (Figure 3B), of which the black, pink, and red modules seen in Figure 3C were most relevant to CAF-S3 cells (Figure 3C). Of these, 921 genes [the black module (427 genes), pink module (255 genes), and red module (239 genes)] were selected as hub CAF-related genes (Figure 3D-F).

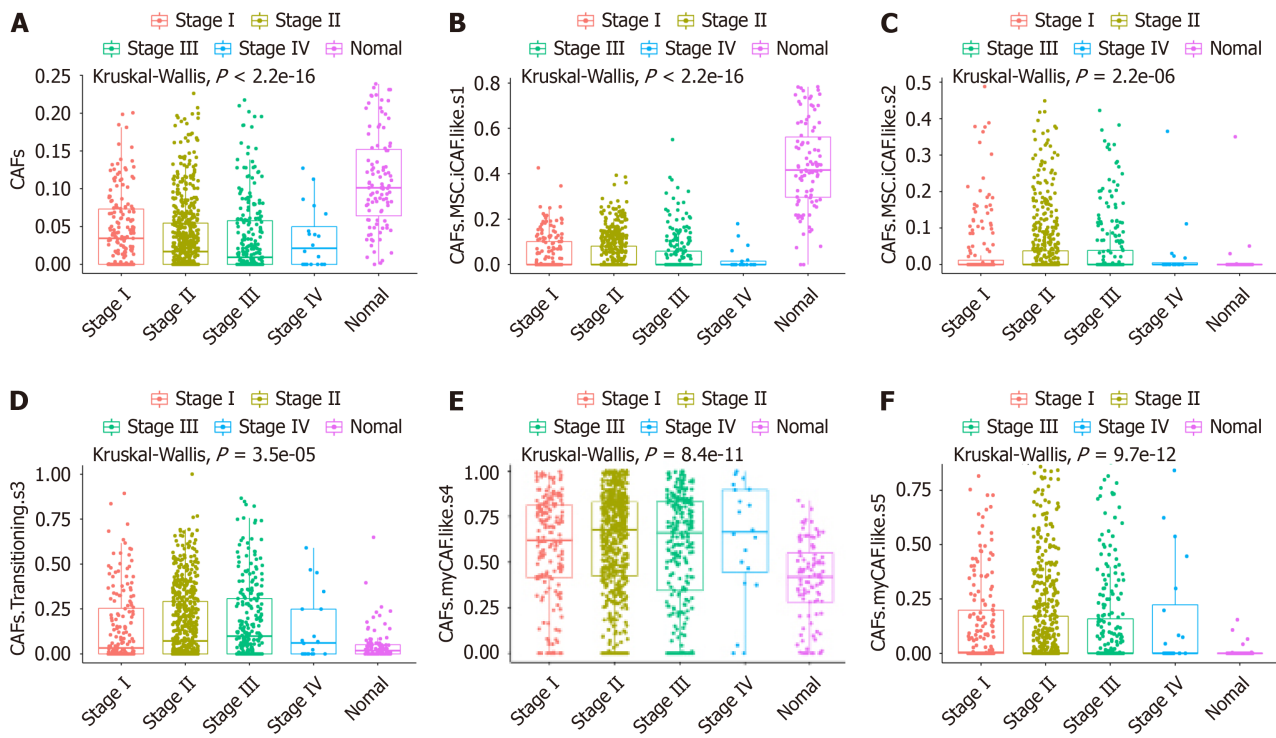
Functional enrichment analysis

GO analysis showed that CAF-related genes were mainly enriched in biological processes related to the ECM and cell adhesion, including focal adhesion, positive regulation of cell adhesion, extracellular structure organization, and ECM organization (Figure 4). KEGG pathway analysis indicated marked enrichment of the genes in pathways associated with cell adhesion (Figure 4).

Screening of prognostic genes and generation of a CAF prognostic gene signature

Only gene expression values greater than 1 were included in this analysis. Univariate analysis showed that 72 CAF-related genes were strongly associated with OS. Further LASSO and multivariate analyses showed that eight CAF-associated genes (IL18, MYD88, GLIPR1, TNN, BHLHE41, DNAJB5, FKBP14, and XG) were independent prognostic factors of BC patient OS (Figure 5A-C).

A risk score (RS) system was established using the expression levels of these eight genes and their corresponding coefficients obtained from the multivariate Cox regression analysis. We then calculated the RS using the formula: RS [CAF prognostic gene signature (CAFPS)] = $(-0.168 \times \text{IL18 levels}) + (-0.420 \times \text{MYD88 levels}) + (-0.338 \times \text{GLIPR1 levels}) + (-$



DOI: 10.12998/wjcc.v12.i4.700 Copyright ©The Author(s) 2024.

Figure 1 Cell fractions of cancer-associated fibroblasts in different cancer stages and normal tissues. A: Cancer associated fibroblasts (CAFs); B: CAFs mesenchymal stem cell (MSC) inflammatory CAF (iCAF)-like s1; C: CAFs MSC iCAF-like s2; D: CAF Transitioning s3; E: CAFs myCAF-like s4; F: CAFs myCAF-like s5.

0.236 × TNN levels) + (-0.129 × BHLHE41 levels) + (-0.577 × DNAJB5 levels) + (0.695 × FKBP14 levels) + (0.573 × XG levels).

Evaluation of biomarkers

Genetic alterations in the biomarkers were assessed using data from the TCGA database. Most of the eight biomarkers exhibited high CNV frequencies in BC (IL18: 37.26%, MYD88: 22.05%, GLIPR1: 17.11%, TNN: 27.76%, BHLHE41: 16.16%, DNAJB5:14.07%, FKBP14: 15.21%, and XG: 14.83%; **Figure 6**).

Predictive accuracy of the eight-gene prognostic signature

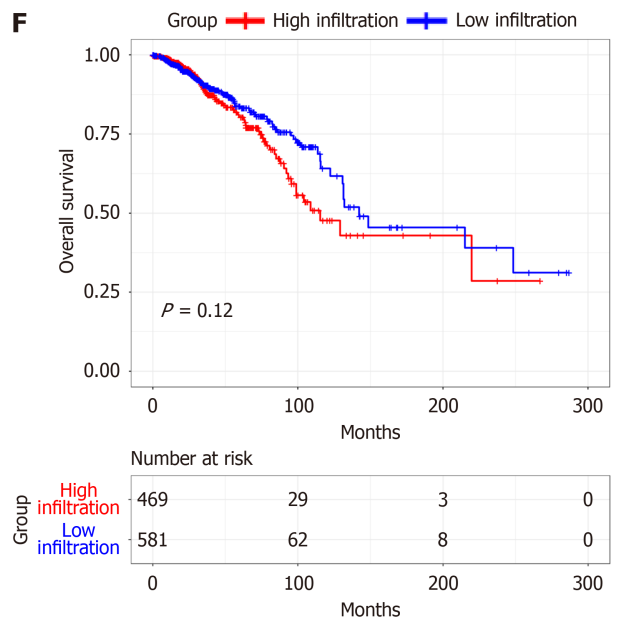
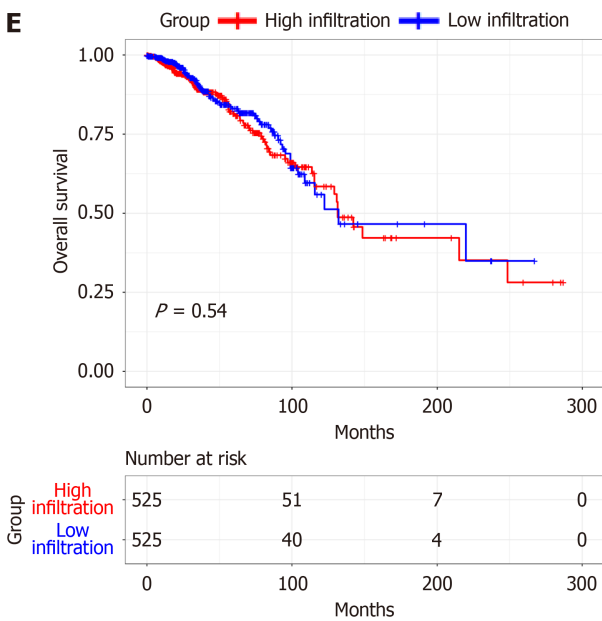
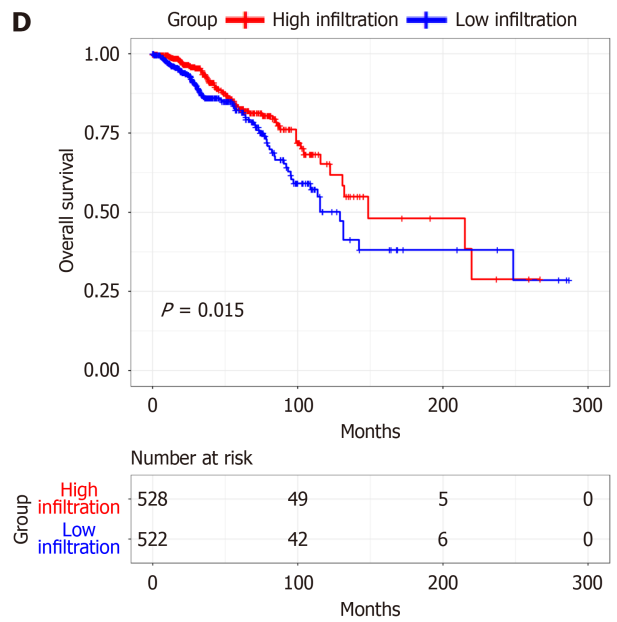
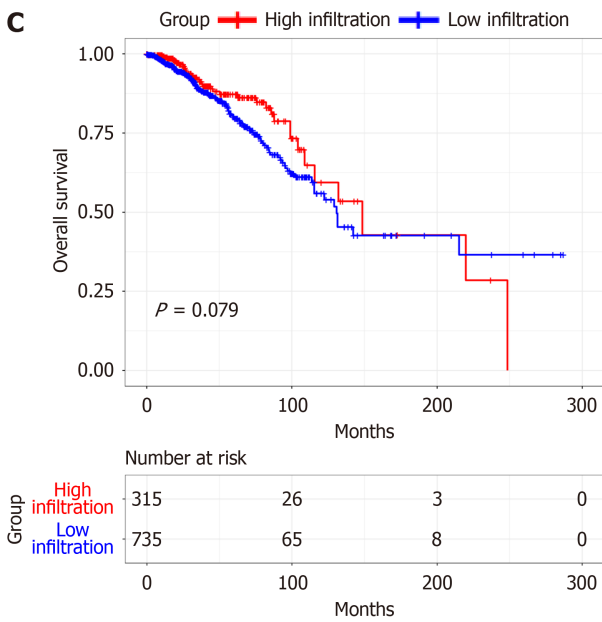
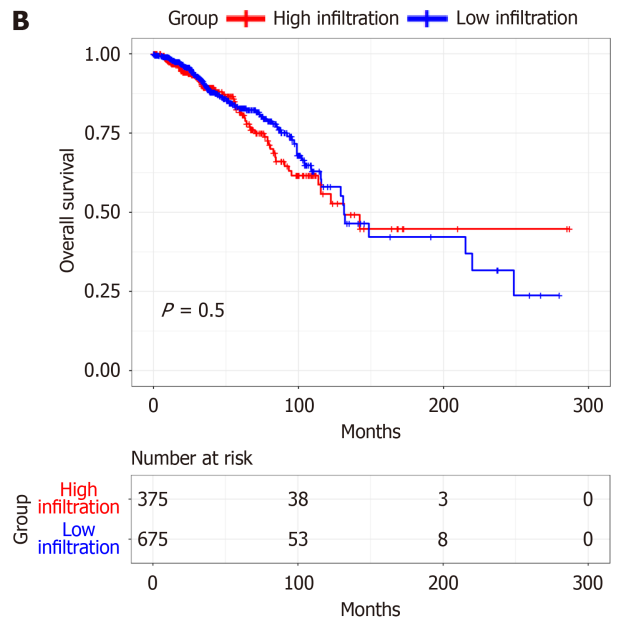
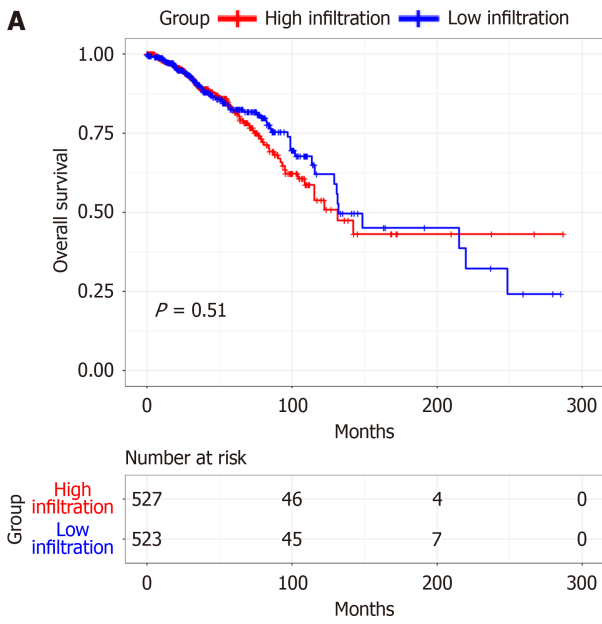
Using the median RS, we separated BC patients into either low- (LR) or high-risk (HR) groups to evaluate the predictive accuracy of the eight-gene prognostic signature. This showed that the LR group had significantly better OS, compared with the HR group (HR 2.951, 95%CI 2.220-3.924, $P < 0.0001$; **Figure 7A**). The AUCs of the prognostic signature showed that it was effective for predicting the OS of patients with BC (3-year AUC = 0.698, 5-year AUC = 0.719, 8-year AUC = 0.752) (**Figure 7B**). We generated risk curves and scatter plots to display the RS and survival status of individual BC patients, finding that poorer outcome was strongly related to an elevated RS (**Figure 7C** and **D**). Furthermore, a heatmap depicting the expression patterns of the risk-associated genes in both groups showed that FKBP14 and XG levels were significantly increased in HR patients, while the levels of IL18, MYD88, GLIPR1, TNN, BHLHE41, and DNAJB5 were elevated in LR patients (**Figure 7E**). Multivariate analysis indicated that the CAFPS was an independent prognostic factor of BC patient prognosis after adjustment for other clinical factors (HR 2.466, 95%CI 1.843-3.298, $P < 0.001$) (**Figure 8**).

The eight-gene prognostic signature was then validated using the GSE96058 and GSE21653 datasets. Kaplan-Meier survival curves confirmed that the HR cohort experienced worse OS relative to the LR cohort (GSE96085 cohort: $P < 0.0001$; GSE21653 cohort: $P = 0.01$) (**Figure 9A** and **B**).

We then investigated whether RS could predict outcomes in various subgroups, including age ≥ 60, age < 60, phase I-II, phase III-IV, TNBC, and non-TNBC. This showed that all subgroups were accurately estimated by RS. Stratification analyses in the TCGA indicated worse OS for HR patients in each stratum, including age, stage, and molecular subtype, compared with LR patients. These data indicated that the CAFPS was a robust and independent predictor of OS in different populations (**Supplementary Figure 2**).

Correlation between the CAFPS and clinicopathological factors

To further assess whether CAF-related genes participated in the development of BC, we assessed the associations between CAFPS and patient clinicopathological factors. This showed that the CAFPS was significantly correlated with pathological T stage, pathological M stage, and molecular subtype (**Figure 10**). The higher the T stage, the higher the corresponding RS. Patients with metastasis and Her2-enrichment had higher RS values.



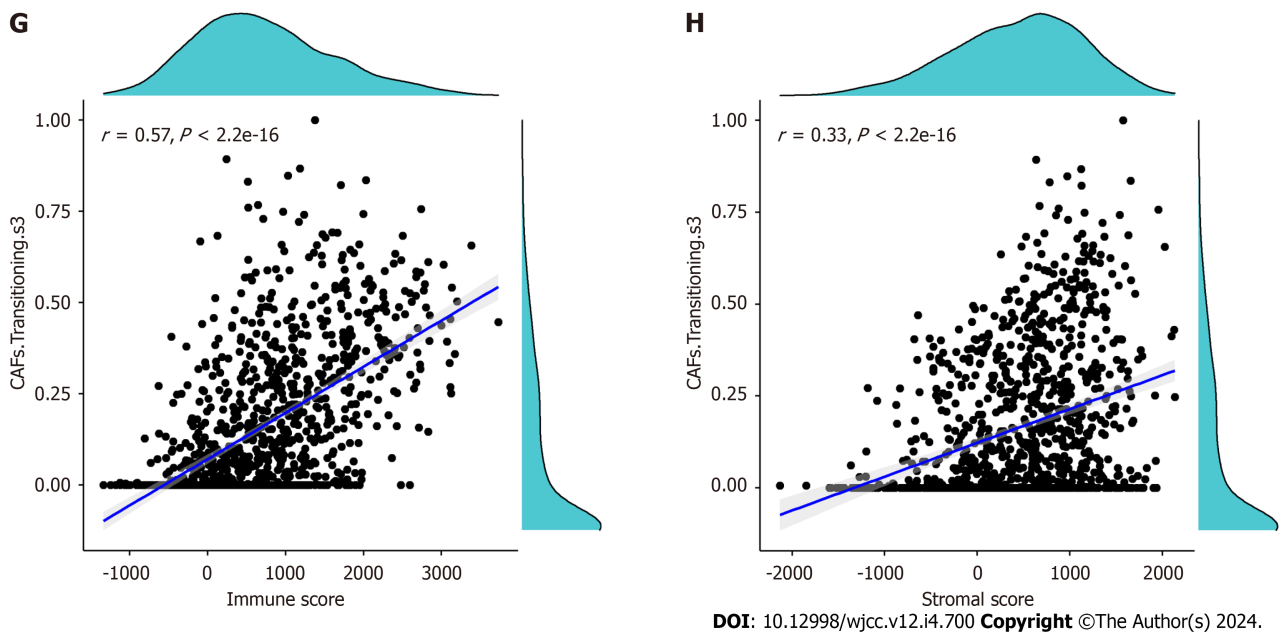


Figure 2 Kaplan-Meier curves of overall survival in relation to cancer associated fibroblasts, and the relationship between the cancer associated fibroblasts transitioning s3 and stromal and immune scores. A: Cancer associated fibroblasts (CAFs); B: CAFs mesenchymal stem cell (MSC) inflammatory CAF (iCAF)-like s1; C: CAFs MSC iCAF-like s2; D: CAFs Transitioning s3; E: CAFs myCAF like s4; F: CAFs myCAF like s5; G-H: The relationship between the CAFs transitioning s3 and the immune and stromal scores.

Generation of the CAFPS-based nomogram

A nomogram was generated using the eight-gene CAFPS and several patient clinical characteristics, namely, age and pathological status, to predict the 3 and 5-year OS of BC patients (Figure 11A). All patients were given a point each for individual prognostic parameters, and a higher total score indicated worse prognosis. We next assessed the predictive efficacy of the nomogram using time-dependent ROC curve analysis. This showed that the AUCs of the nomogram were 0.805 and 0.801 for the 3- and 5-year OS rate predictions, respectively (Figure 11B and C). Moreover, higher AUCs were seen compared with the pathological stage. These results demonstrated the satisfactory predictive efficacy of the nomogram in determining the outcomes of BC patients (Figure 11D and E).

Prognostic value of CAFPS in relation to drug response

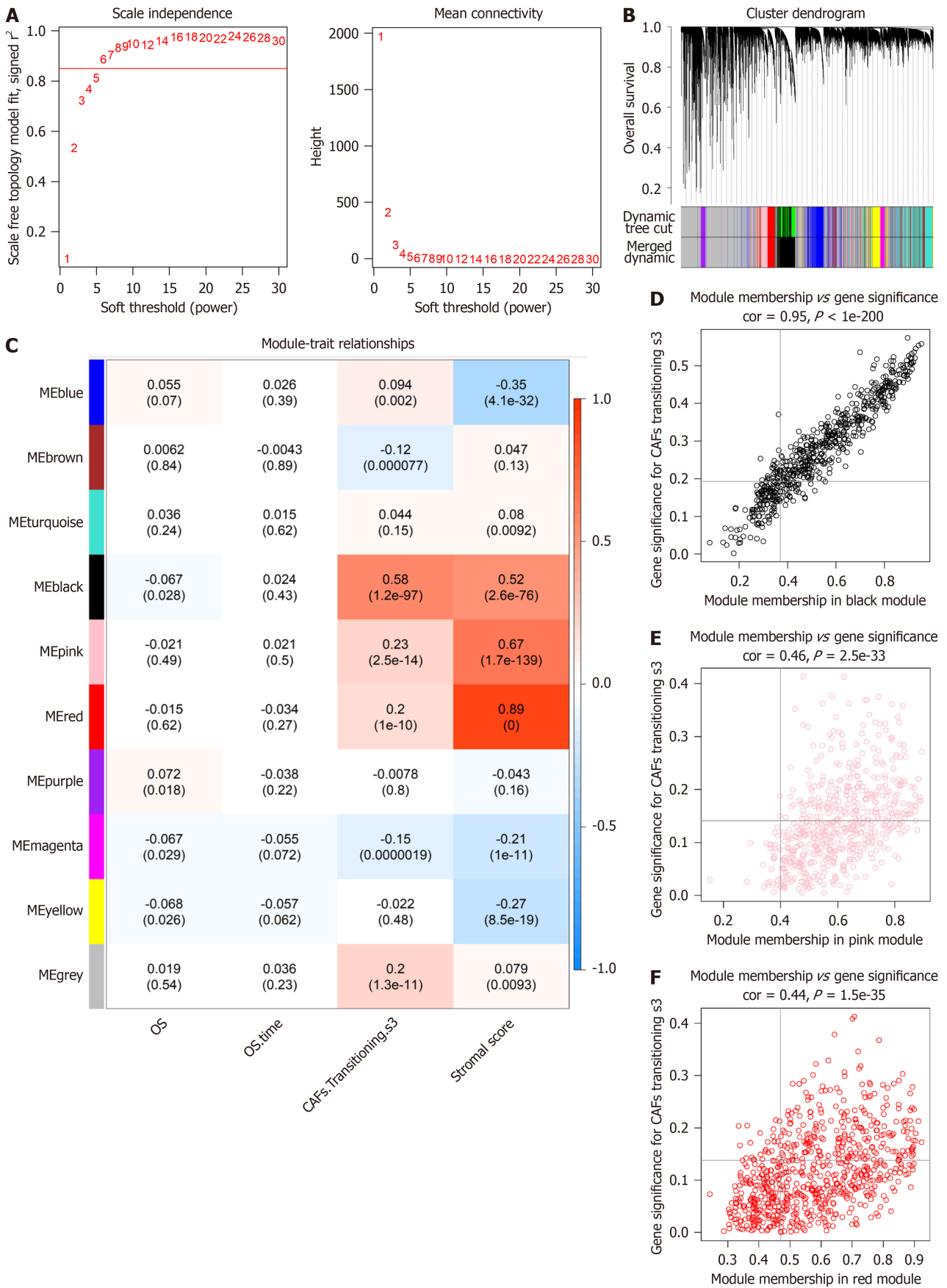
Patients in the GSE18728 dataset underwent chemotherapy. Of these, 11 responded while 17 did not. The CAFPS scores of the patients who responded were significantly lower compared to those of the non-responding patients (Wilcoxon test, $P = 0.048$, Figure 12A). Moreover, patients with reduced CAFPS scores responded better than those with elevated scores (Figure 12B). These findings indicate that the CAFPS was effective for estimating patient response to chemotherapy. This also explained the worse outcome and rapid cancer progression of patients with elevated CAFPS scores who underwent chemotherapy.

Evaluation of the prognostic gene signature, immune checkpoints, and hallmark gene networks

We next assessed differences in the levels of immune checkpoint molecules between the HR and LR cohorts. Relative to the HR cohort, the levels of PDCD1 (PD1) ($P < 2.22e-16$), CD274 (PD-L1) ($P < 2.22e-16$), CTLA4 ($P < 2.22e-16$), LAG3 ($2.7e-13$), IDO1 ($P < 2.22e-16$), and TIGIT ($P < 2.22e-16$) were significantly raised in the LR cohort (Figure 13). Another interesting finding was that almost all of the hallmark gene networks were significantly associated with CAFPS (Figure 14A). Moreover, the single-sample gene set enrichment analysis (ssGSEA) showed that the CAFPS RS was negatively associated with the TGF-BETA ($r = -0.091$, $P = 0.0032$), IL-6-JAK-STAT3 ($r = -0.37$, $P < 2.2e-16$), and TNFA-SIGNALING-VIA-NFKB ($r = -0.34$, $P < 2.2e-16$) signaling pathways (Figure 14B-D).

External experimental validation of prognostic signature

We found that the expression levels of FKBP14 was significantly higher in breast cancer samples than in the paired adjacent normal tissues. Patients were divided into high expression group and low expression group based on the median values of FKBP14 expression. Among patients with high FKBP14 expression, the proportion of patients with tumor size > 2 cm, lymph node metastasis and TNM stage III was higher than that of patients with low FKBP14 expression ($P < 0.05$) (Table 2).



DOI: 10.12998/wjcc.v12.i4.700 Copyright ©The Author(s) 2024.

Figure 3 Co-expression pathways generated by weighted gene co-expression network analysis. A: A soft-thresholding power (β) of 6 was chosen, following the scale-free topology criterion; B: Clustering dendrograms depicting genes with comparable expression signatures were grouped into co-expression modules; C: Module-trait associations illustrating the relationships between individual gene module eigengenes and matching phenotype; D-F: Scatter plots of the

module membership and gene significance of individual genes in the black, pink, and red modules.

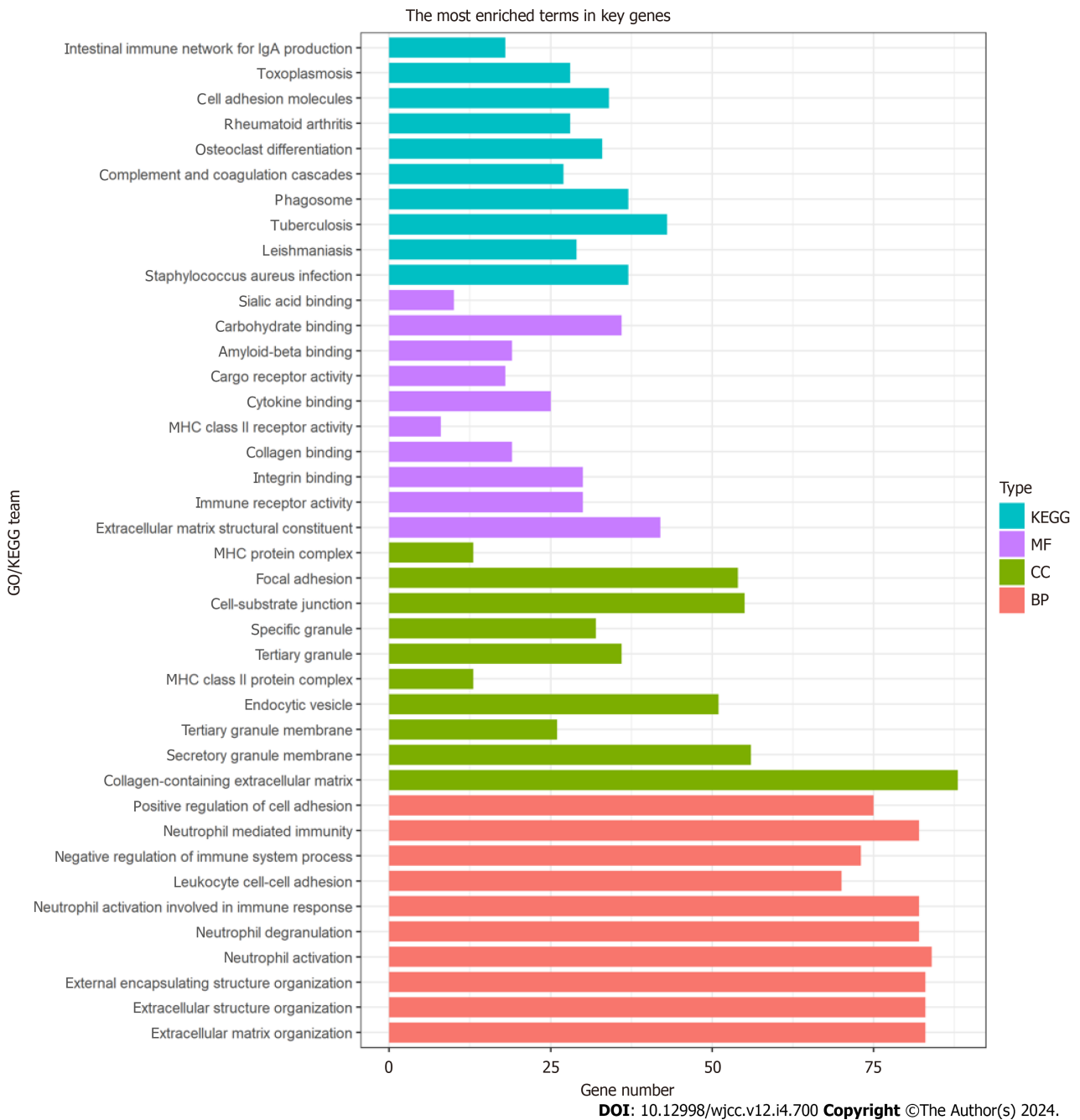


Figure 4 Gene ontology and Kyoto Encyclopedia of Genes and Genomes enrichment analyses. The gene ontology analysis of enriched biological process, cellular component, and molecular function terms, and the Kyoto Encyclopedia of Genes and Genomes analysis of hub genes. KEGG: Kyoto Encyclopedia of Genes and Genomes; MF: Molecular function; CC: Cellular component; BP: Biological process.

DISCUSSION

Current methods are relatively ineffective for predicting the outcomes of BC patients, likely due to complications related to phenotypes and underlying mechanisms. However, advances in bioinformatics have allowed the identification of new biomarkers to aid BC diagnosis and the estimation of patient outcomes[22,23]. CAFs, non-neoplastic stromal cells found within the TME, aid in tumor formation and metastasis[24,25]. Multiple studies have identified CAFs as indicators of drug resistance and worse outcome in a range of tumors[26-28]. Moreover, it was revealed that factors secreted by CAFs can transmit signals to tumor cells that promote drug resistance[29]. Furthermore, CAFs also release cytokines, exosomes, and growth factors, which influence components of the TME, thereby modulating the therapeutic response. Emerging evidence has revealed a strong association between the number and activity of CAFs and patient prognosis[13,14,28].

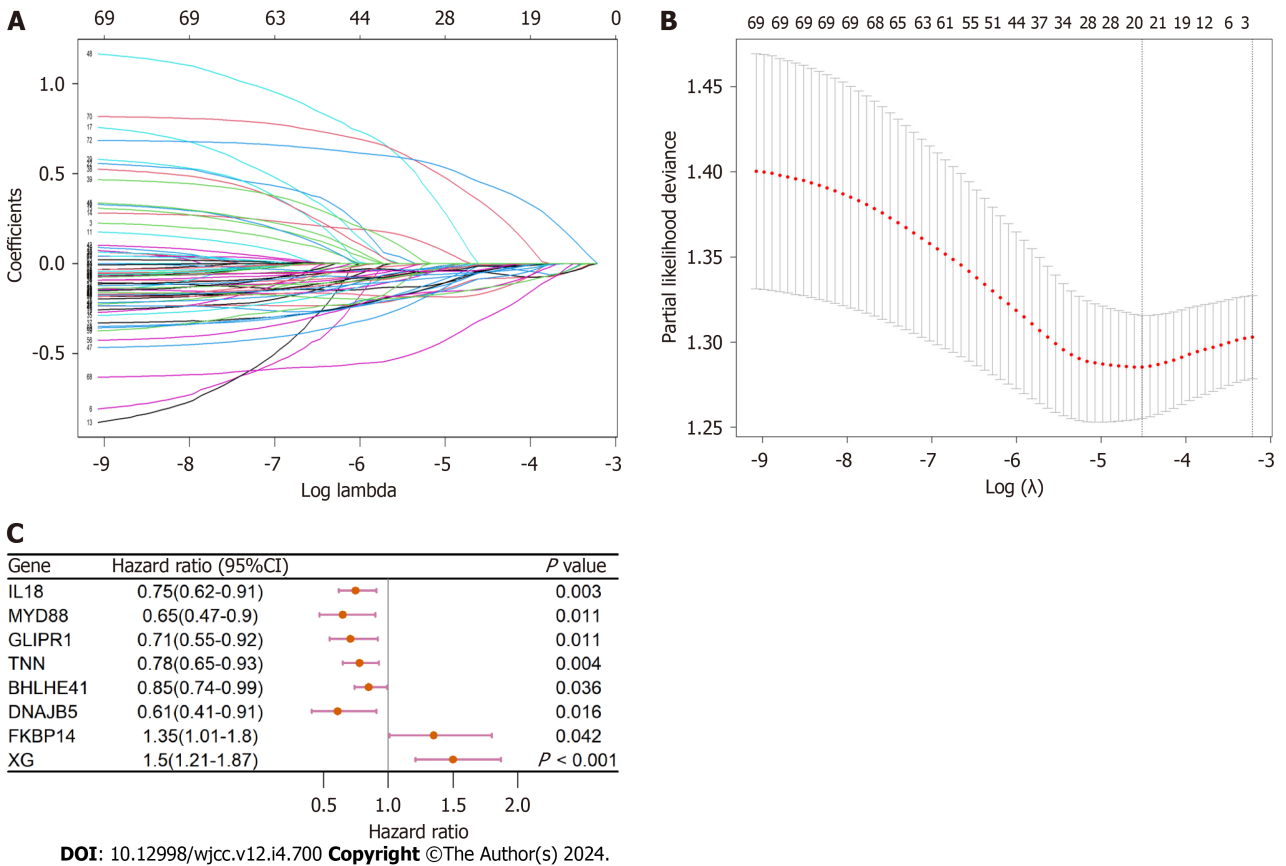


Figure 5 The mechanism of variable selection. A and B: The performance of least absolute shrinkage and selection operator (LASSO) analysis; C: Forest plot of multivariate analysis for the establishment of the prognostic signature.

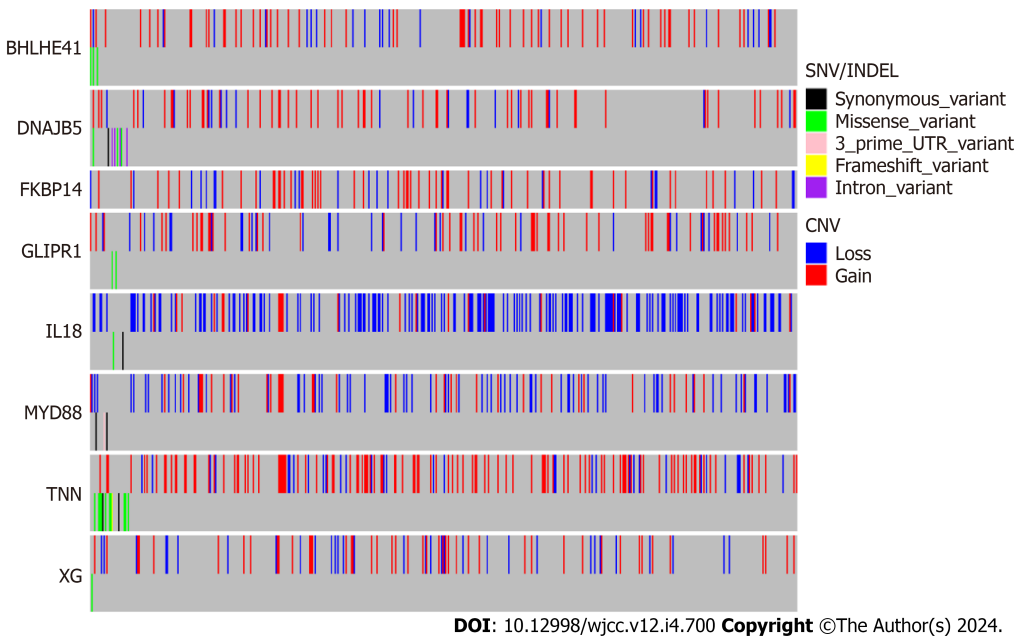
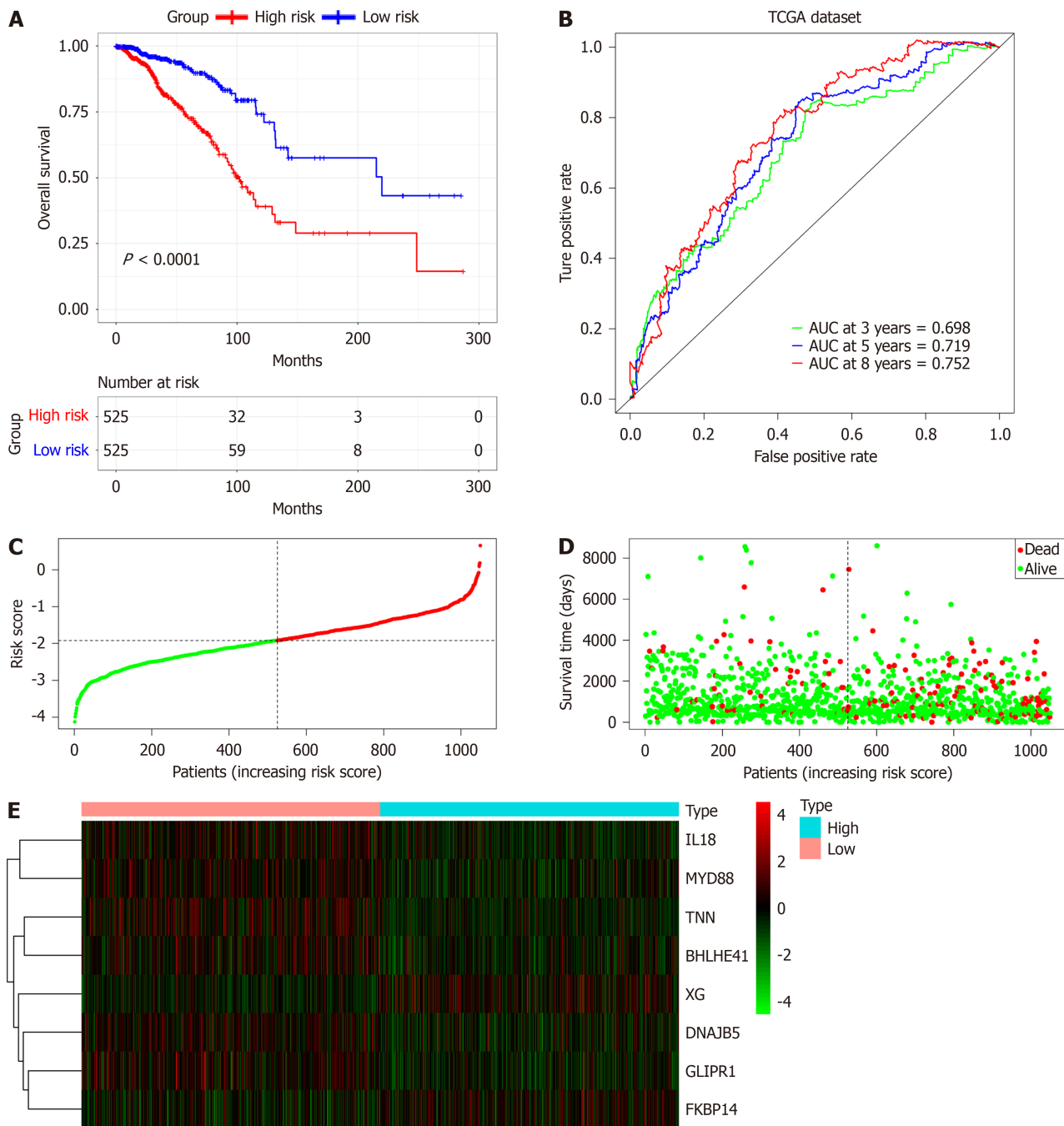


Figure 6 Mutation and copy number alteration analysis of the hub genes. CAN: Copy number alteration.

Hence, targeting CAFs may be beneficial to anti-cancer therapy.

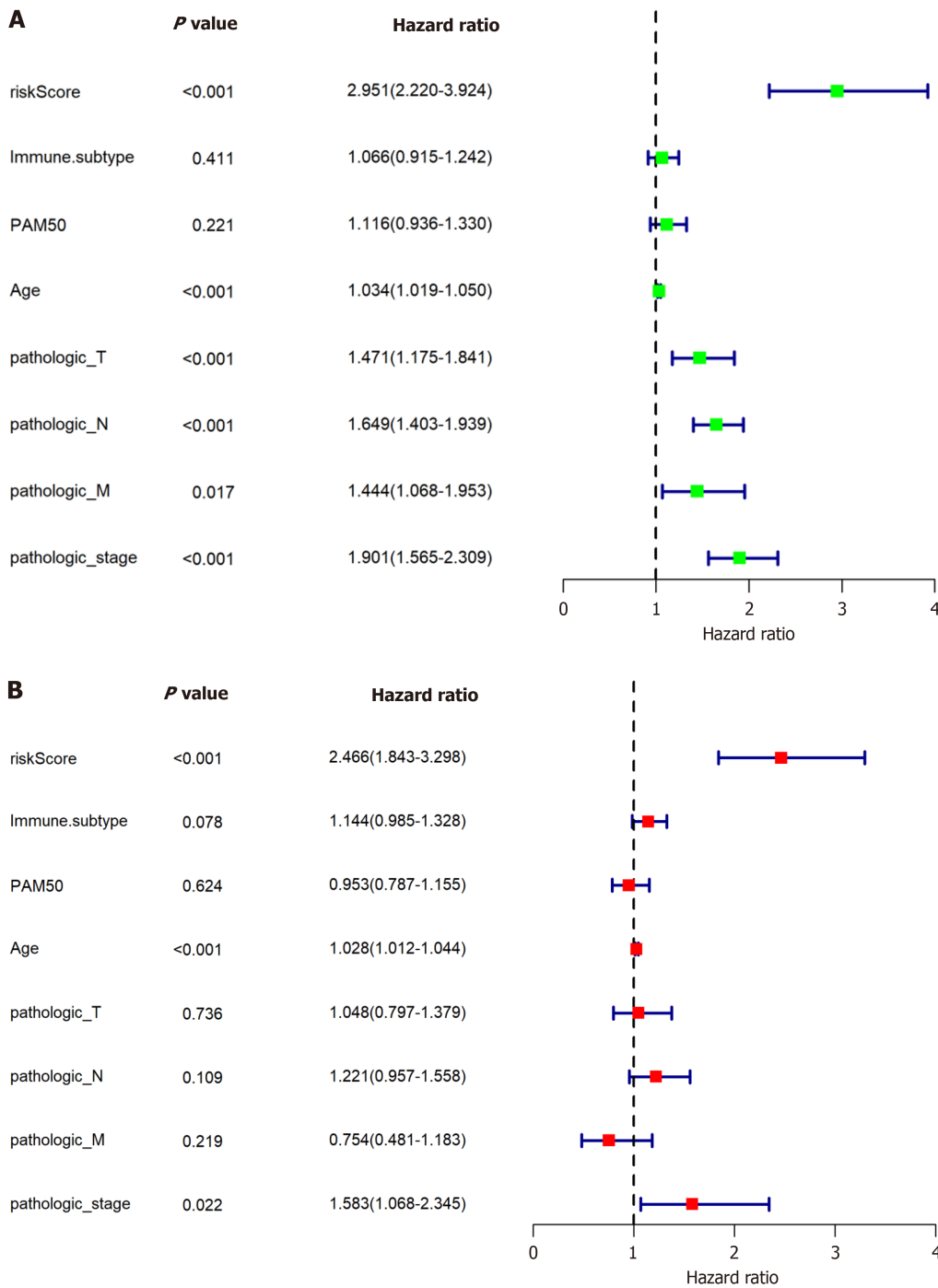
Prior investigations have identified fibroblasts based on their expression of FAP and α SMA[30]. However, fibroblasts are distinct from cancer cells and have thus not been further stratified. Single-cell RNA sequencing (scRNA-seq) can examine the entire cellular signature of tumor cells[31,32]. Recent CAF examinations recognized two polarized states regulated by ECM formation or inflammatory secretomes[33-35].



DOI: 10.12998/wjcc.v12.i4.700 Copyright ©The Author(s) 2024.

Figure 7 Evaluation of the prognostic signature using the The Cancer Genome Atlas database. A: Kaplan-Meier plots of overall survival between the high- and low-risk cohorts; B: Time-dependent receiver operating characteristic curve analysis; C: Risk score distribution; D: Survival distribution; E: Expression heatmap of the 8 cancer associated fibroblast-associated risk genes.

Previous reports indicated that cancer-associated fibroblast genes expression can estimate breast cancer patient prognosis and predict the responses to immunotherapy[36-38]. Wang *et al*[36] reported that signature based on cancer-associated fibroblast genes could divide patients into low- and high-risk groups, accompanied by different OS, clinical features, and immune infiltration characteristics. Huang *et al*[37] identified various heterogeneous CAF cell populations in breast cancer patients. An CAF-associated gene signature was developed to predict the responses to immunotherapeutics. The five-gene prognostic CAF signature presented by Xu *et al*[38] was effective in estimating clinical immunotherapy response. In this study, we confirmed that the proportion of CAF-S3 cells was closely associated with patient prognosis, based on the CAF-related gene expression signature obtained from previous reports[16]. Subsequently, we regarded the proportion of CAF-S3 cells as a clinical characteristic and developed a CAF-based gene signature using eight genes (IL18, MYD88, GLIPR1, TNN, BHLHE41, DNAJB5, FKBP14, and XG) using WGCNA, univariate, LASSO, and multivariate analyses to predict patient prognosis. This demonstrated that the LR cohort had markedly better OS compared with the HR cohort. AUC analysis of the prognostic signature demonstrated its accuracy in predicting the OS of patients with breast cancer. Furthermore, multivariate analysis showed that the signature was an independent prognostic



DOI: 10.12998/wjcc.v12.i4.700 Copyright ©The Author(s) 2024.

Figure 8 Assessment of the independent prognostic value of the prognostic signature using the The Cancer Genome Atlas database. A: Univariate analyses of the signature and clinical features; B: Multivariate analyses of the signature and clinical features.

factor. The CAFPS OS predictive efficacy was further validated using the GSE96058 and GSE21653 datasets from the GEO and subgroups of the TCGA databases. These findings indicate that the CAFPS was a reliable predictor of BC patient prognosis.

We then generated a nomogram to estimate BC patient outcomes. Based on our results, our model was highly effective in predicting BC patient prognosis. The results of the calibration curves demonstrated that the nomogram was able to accurately predict the prognosis of patients with BC. However, when compared with traditional clinical features, the prognostic signature showed even better potential for clinical application. According to the model, a reduced CAFPS RS was significantly related to enhanced chemotherapeutic response in BC patients. In addition, CAFPS was strongly correlated with most hallmark gene sets, explaining the rapid progression and worse outcomes of patients with elevated CAFPS values. Immune checkpoint molecules can also reflect the immune status of tumor microenvironments. In the present study, the levels of immune checkpoint molecules were found to be significantly elevated in the LR cohort, implying that patients with low CAFPS RS may respond better to immune checkpoint therapy.

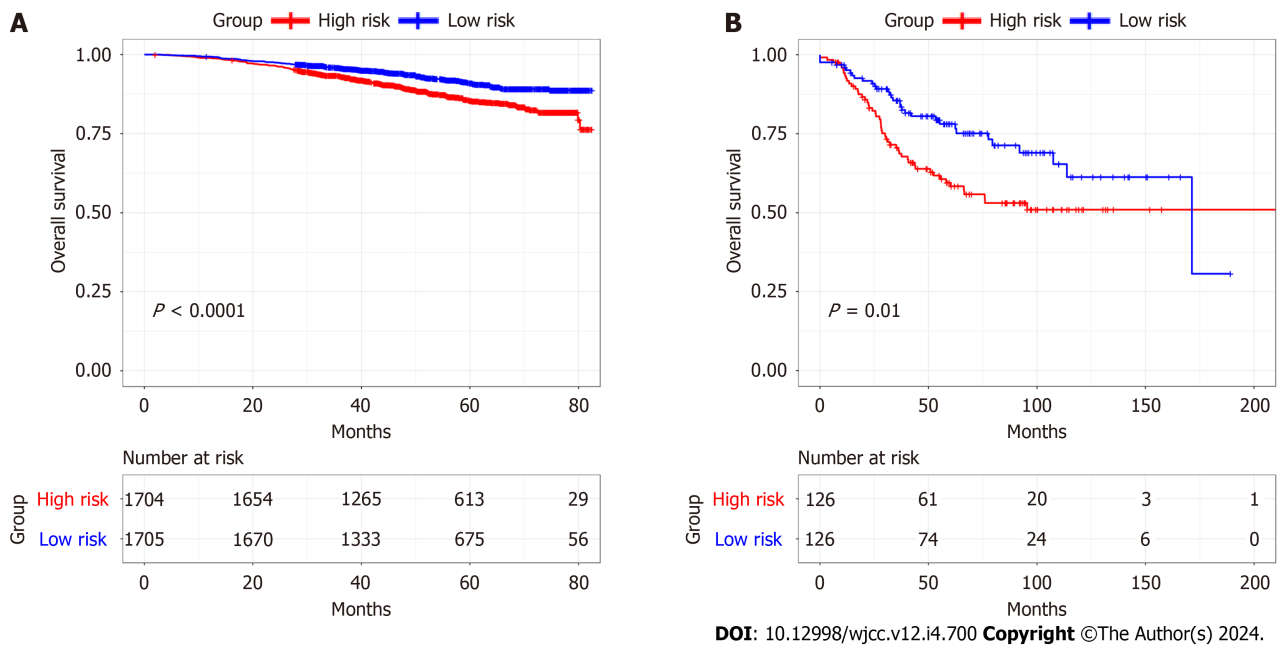


Figure 9 Validation of the prognostic signature. A: Kaplan-Meier plots of overall survival of high- and low-risk cohorts in the GSE96058 database; B: Kaplan-Meier plots of overall survival of high- and low-risk cohorts in the GSE21653 database.

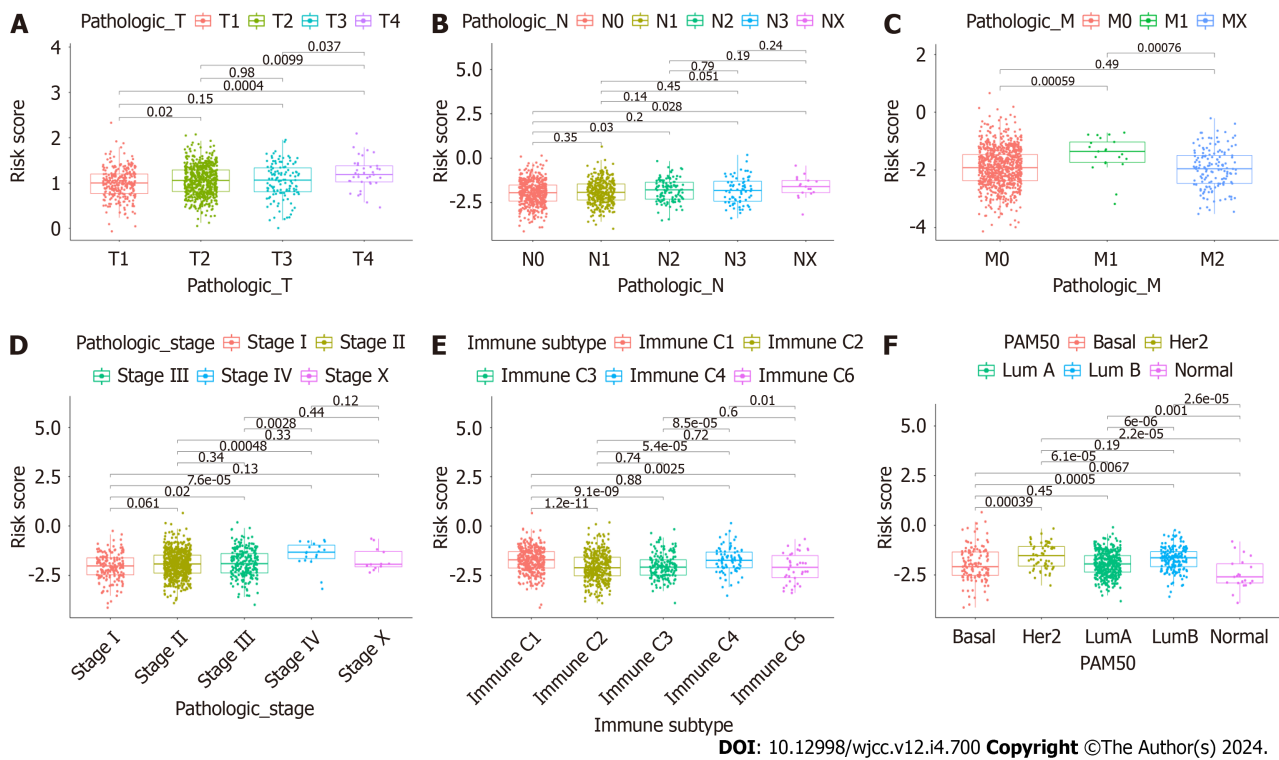


Figure 10 Association between CAFPS and clinicopathological factors. A: Pathologic-T; B: Pathologic-N; C: Pathologic-M; D: Pathologic-stage; E: Immune subtype; F: PAM50.

For a proper evaluation of the prognostic signature, we then assessed individual biomarkers. IL-18 is a member of the IL-1 family of proinflammatory cytokines. IL-18 modulates Th1 and Th2 immune responses, as well as the activation of NK cells and macrophages[39]. It is reported that the IL-18 protein is strongly expressed in human BC and lymph node tissues, and is directly associated with lymph node metastasis in BC[40]. MYD88 serves a critical function in both innate and adaptive immune responses. It is also involved in crosstalk with the interleukin-1 and Toll-like receptor networks. MYD88 expression is high in metastatic tumors and has been suggested as a potential therapeutic target[41]. GLIP1R1 is markedly up-regulated in BC and has been identified as an oncoprotein in BC. In BC cells, GLIP1R1 expression is promoted by prolactin and estrogen, promoting cell proliferation[42]. TNN is abundantly expressed in human breast tumor

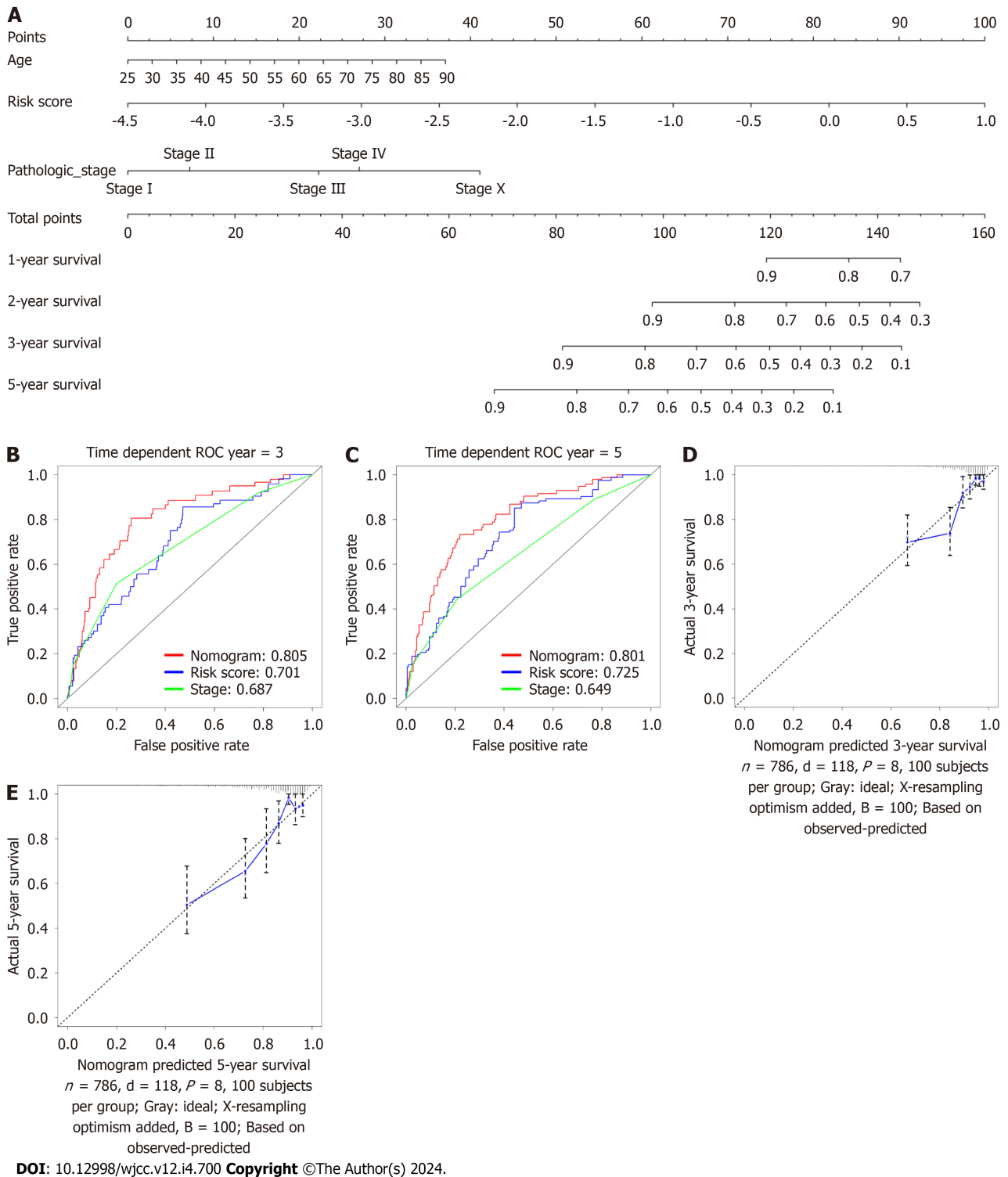


Figure 11 Nomogram generation for the prediction of 3- and 5-year survival. A: Development of a nomogram for estimating 1-, 2-, 3- and 5-year survival probabilities of breast cancer patients using the The Cancer Genome Atlas (TCGA) database; B and C: The 3- and 5-year area under the curves of nomogram, stage, CAFPS using the TCGA database; D and E: The 3- and 5-year calibration curves for predicting overall survival.

extracts, although it is absent in adjoining normal tissue. Therefore, it is possible that TNN promotes tumor development by inducing BC cell migration[43]. BHLHE41 is a critical modulator of the invasive and metastatic phenotype in triple-negative BC. It is modulated by the p63 metastasis suppressor, and it suppresses TNBC aggressiveness by inhibiting hypoxia-inducible factor 1a (HIF-1a) and HIF-2a (HIFs)[44]. DNAJB5 belongs to the DnaJ/heat shock protein 40 (HSP40) family, and it partners with HSP70 chaperones. Stable DNAJB5 expression in cholangiocarcinoma cells that overexpress microRNA 21 re-sensitizes them to HSP90 inhibitors[45]. FKBP14 is a member of the FK506-binding protein (FKBP) family and is highly expressed in gastric cancer. Patients with elevated FKBP14 Levels typically have poor outcomes. FKBP14 is recognized as an oncogene in gastric cancer and has the potential as a marker for gastric cancer identification, invasion, and prognosis[46]. Relative to normal tissues, FKBP14 is ubiquitously expressed in ovarian cancer tissues where

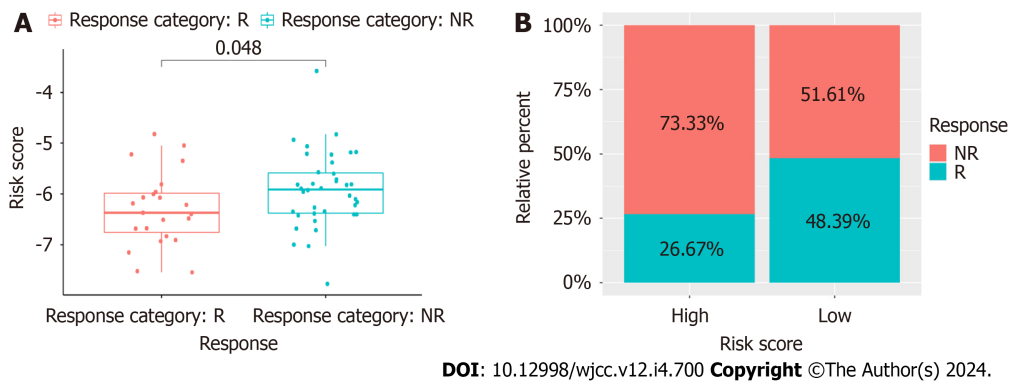


Figure 12 Prediction of chemotherapy response. A: The cancer associated fibroblast risk score of estimated chemotherapy-responders and non-responders in GSE18728; B: Distributions of responders and non-responders in high- and low-risk groups in GSE18728.

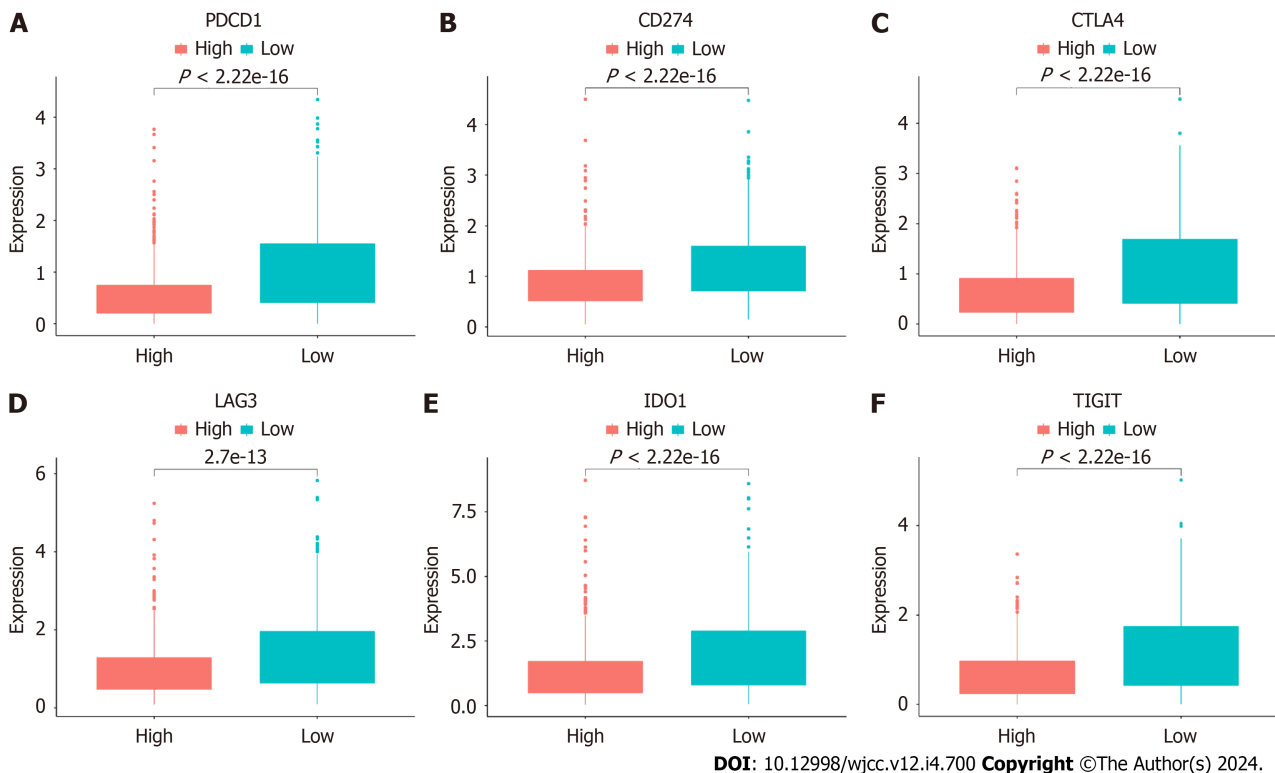


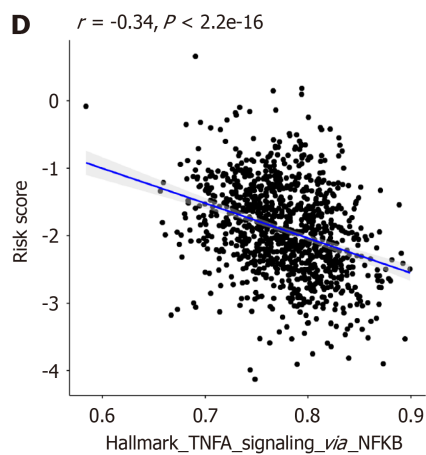
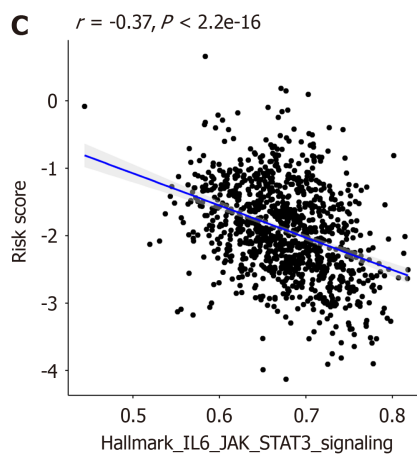
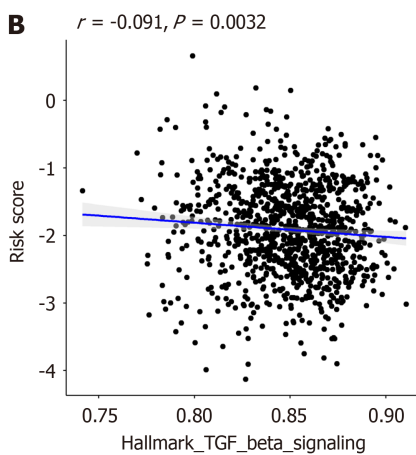
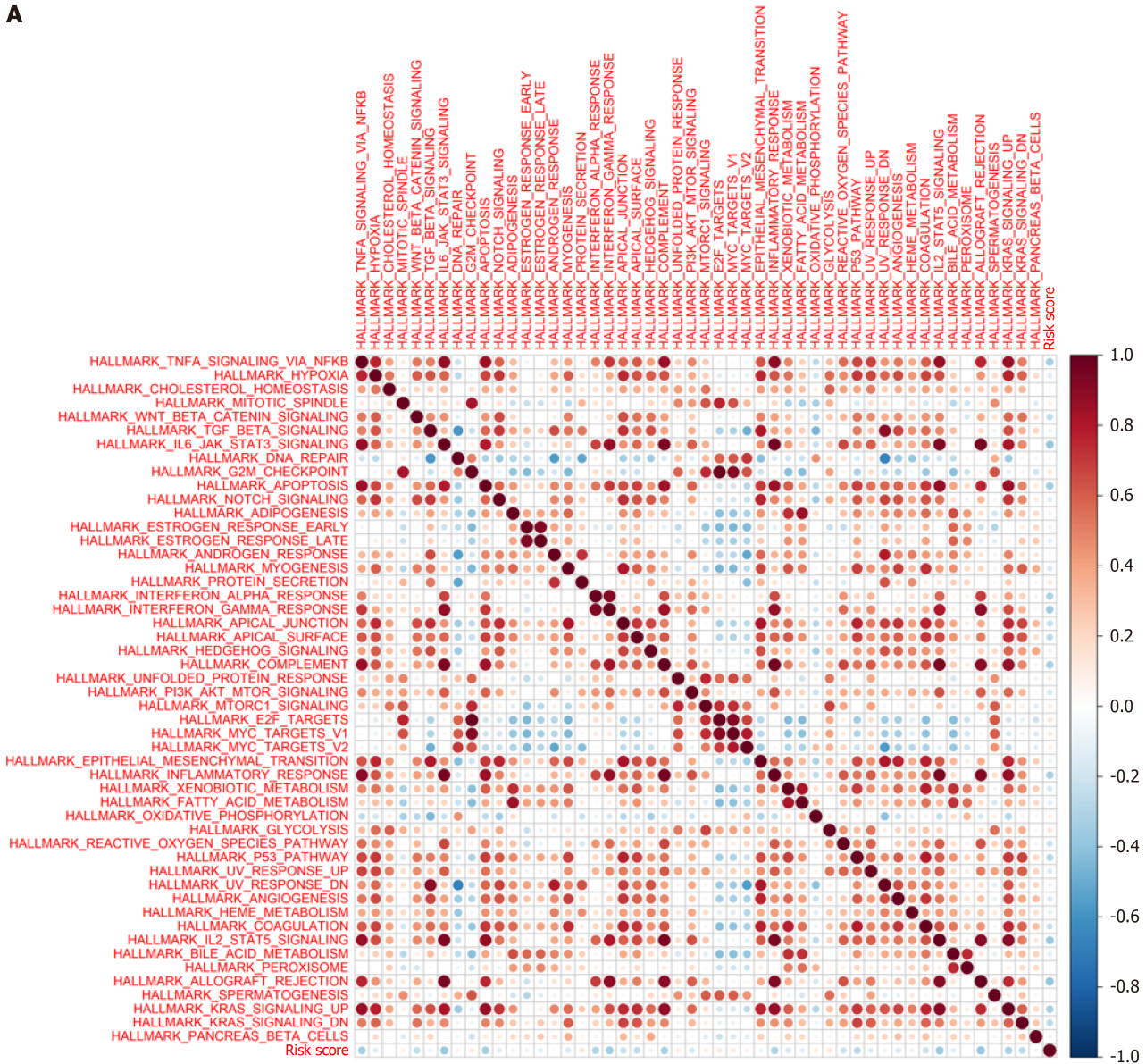
Figure 13 Immune checkpoint gene expression in both risk cohorts in The Cancer Genome Atlas cohort. A: PDCD1; B: CD274; C: CTLA4; D: LAG3; E: IDO1; F: TIGIT.

it was shown to be indicative of tumor size and grade in ovarian cancer tissues[47]. In our study, Among patients with high FKBP14 expression, the proportion of patients with tumor size > 2 cm, lymph node metastasis and TNM stage III was higher than that of patients with low FKBP14 expression. XG belongs to the CD99 family and its expression has been correlated with worse OS in Ewing's sarcoma patients with benign tumors, and it is speculated to regulate metastasis. Moreover, we further verified the abnormal expression of the risk genes (FKBP14) through experiments. Nevertheless, there is very limited information regarding the function of CAFs in BC. Hence, it is critical to conduct additional investigations into the eight CAF-related gene markers and their associated underlying mechanisms to better elucidate infiltration, metastasis, and drug resistance in BC patients. Our research has several limitations: (1) The size of our analyzed dataset was relatively small, and a larger patient population must be studied to validate our results; and (2) This paper did not go into detail regarding the mechanism associated with the eight identified genes.

CONCLUSION

Here, we generated a CAF-associated gene prognostic signature using IL18, MYD88, GLIPR1, TNN, BHLHE41, DNAJB5, FKBP14, and XG as prognostic markers of BC. This novel signature can be employed to estimate BC patient outcomes

A



DOI: 10.12998/wjcc.v12.i4.700 Copyright ©The Author(s) 2024.

Figure 14 Correlation between CAFPS and signaling pathways. A: Spearman's correlation analyses revealing that CAFPS is significantly correlated with most hallmark gene sets; B: The ssGSEA data revealing that the cancer associated fibroblast (CAF) risk score is directly associated with TGF-BETA signaling pathways enrichment scores using The Cancer Genome Atlas (TCGA) database; C: The ssGSEA data revealing that the CAF risk score is directly associated with IL-6-JAK-STAT3 signaling pathways enrichment scores using the TCGA database; D: The ssGSEA data revealing that the CAF risk score is directly associated with The TNFA-SIGNALING-VIA-NFKB signaling pathways enrichment scores using the TCGA database.

Table 1 Clinical and pathological characteristics of patients with breast cancer in The Cancer Genome Atlas cohort

Variables	<i>n</i>	%
Age, yr		
< 60	570	53.17
≥ 60	571	46.74
NA	1	0.09
Pathologic-T		
T1	274	25.56
T2	621	57.93
T3	133	12.41
T4	40	3.73
TX	4	0.37
Pathologic-N		
N0	502	46.83
N1	355	33.12
N2	118	11.01
N3	76	7.08
NA	21	1.96
Pathologic-M		
M0	896	83.58
M1	22	2.05
NA	154	14.37
Stage		
Stage I	176	16.41
Stage II	608	56.72
Stage III	246	22.95
Stage IV	20	1.87
NA	22	2.05
PAM50		
Basal	136	12.69
Luminal-A	413	38.53
Luminal-B	185	17.25
Her2	66	6.16
Normal	22	2.05
NA	250	23.32

Table 2 Relationship between expression level of FKBP14 and clinical features in breast cancer

Variables	<i>n</i>	Low expression of FKBP14 (<i>n</i> = 40)	High expression of FKBP14 (<i>n</i> = 40)	χ^2	<i>P</i> value
Age (yr)					
≤ 60	53	27 (67.5)	26 (65)	0.056	0.813
> 60	27	13 (32.5)	14 (35)		
Tumor size					
				10.769	0.002

≤ 2 cm	28	21 (52.5)	7 (17.5)		
> 2 cm	52	19 (47.5)	33 (82.5)		
Lymph node metastasis				25.208	< 0.001
No	48	35 (87.5)	13 (32.5)		
Yes	32	5 (12.5)	27 (67.5)		
Stage				11.250	0.001
I-II	64	38 (95)	26 (65)		
III	16	2 (5)	14 (35)		
Subtype				3.660	0.056
Triple negative	17	12 (30)	5 (12.5)		
Non-triple negative	63	28 (70)	35 (87.5)		

conveniently and accurately. These results provide a basis for further studies on the role of CAFs in BC.

ARTICLE HIGHLIGHTS

Research background

Breast cancer (BC), a leading malignant disease, affects women all over the world. It is still urgent to explore new biomarkers to estimate and enhance prognosis of BC patients.

Research motivation

The present study for the first time investigated the 8 cancer associated fibroblasts (CAF)-associated genes as the potential biomarkers of the prognosis of patients using bioinformatics.

Research objectives

This study aims to establish a CAFs-associated prognostic signature to improve BC patient outcome estimation.

Research methods

We retrieved the transcript profile and clinical data of 1072 BC samples from The Cancer Genome Atlas (TCGA) databases, and 3661 BC samples from the The Gene Expression Omnibus. CAFs and immune cell infiltrations were quantified using CIBERSORT algorithm. CAF-associated gene identification was done by weighted gene co-expression network analysis. A CAF risk signature was established *via* univariate, LASSO regression, and multivariate Cox regression analyses. The receiver operating characteristic (ROC) and Kaplan-Meier curves were employed to evaluate the predictability of the model. Subsequently, a nomogram was developed with the risk score and patient clinical signature. Using Spearman's correlations analysis, the relationship between CAF risk score and gene set enrichment scores were examined.

Patient samples were collected to validate gene expression by quantitative real-time polymerase chain reaction (qRT-PCR).

Research results

Employing an 8-gene (IL18, MYD88, GLIPR1, TNN, BHLHE41, DNAJB5, FKBP14, and XG) signature, we attempted to estimate BC patient prognosis. Based on our analysis, high-risk patients exhibited worse outcomes than low-risk patients. Multivariate analysis revealed the risk score as an independent indicator of BC patient prognosis. ROC analysis exhibited satisfactory nomogram predictability. The AUC showed 0.805 at 3 years, and 0.801 at 5 years in the TCGA cohort. We also demonstrated that a reduced CAF risk score was strongly associated with enhanced chemotherapeutic outcomes. CAF risk score was significantly correlated with most hallmark gene sets. Finally, the prognostic signature were further validated by qRT-PCR.

Research conclusions

We introduced a newly-discovered CAFs-associated gene signature, which can be employed to estimate BC patient outcomes conveniently and accurately.

Research perspectives

The mechanisms of 8 CAFs-associated genes in BC is still unclear, which needs further confirmation through molecular biology and clinical experiments.

ACKNOWLEDGEMENTS

The authors thank TCGA and GEO for sharing the BC data.

FOOTNOTES

Co-first authors: Zi-Zheng Wu and Yuan-Jun Wei.

Author contributions: Han M conceived and designed the study and reviewed the manuscript; Wu ZZ, Wei YJ and Zheng J collected, arranged, and analyzed the data and wrote the manuscript; Li T, Liu YF designed and prepared the figures and tables; All authors reviewed and approved the final manuscript. The reasons for designating Wu ZZ and Wei YJ as co-first authors are threefold. First, the research was performed as a collaborative effort, and the designation of co corresponding authorship accurately reflects the distribution of responsibilities and burdens associated with the time and effort required to complete the study and the resultant paper. This also ensures effective communication and management of post-submission matters, ultimately enhancing the paper's quality and reliability. Second, the overall research team encompassed authors with a variety of expertise and skills from different fields, and the designation of co-first authors best reflects this diversity. This also promotes the most comprehensive and in-depth examination of the research topic, ultimately enriching readers' understanding by offering various expert perspectives. Third, Wu ZZ and Wei YJ contributed efforts of equal substance throughout the research process. The choice of these researchers as co-first authors acknowledges and respects this equal contribution, while recognizing the spirit of teamwork and collaboration of this study. In summary, we believe that designating Wu ZZ and Wei YJ as co-first authors of is fitting for our manuscript as it accurately reflects our team's collaborative spirit, equal contributions, and diversity.

Institutional review board statement: This study was reviewed and approved by the Ethics Committee of the First Hospital of Qinhuangdao.

Informed consent statement: All study participants or their legal guardians provided written informed consent before study enrollment.

Conflict-of-interest statement: All the authors report no relevant conflicts of interest for this article.

Data sharing statement: Publicly available datasets were analyzed in this study, these can be found in Xena (<https://xenabrowser.net>), GEO database (www.ncbi.nlm.gov/geo; GSE96058, GSE18728, and GSE21653).

Open-Access: This article is an open-access article that was selected by an in-house editor and fully peer-reviewed by external reviewers. It is distributed in accordance with the Creative Commons Attribution NonCommercial (CC BY-NC 4.0) license, which permits others to distribute, remix, adapt, build upon this work non-commercially, and license their derivative works on different terms, provided the original work is properly cited and the use is non-commercial. See: <https://creativecommons.org/licenses/by-nc/4.0/>

Country/Territory of origin: China

ORCID number: Zi-Zheng Wu 0000-0001-8253-0352; Meng Han 0000-0003-1752-7442.

S-Editor: Liu JH

L-Editor: A

P-Editor: Xu ZH

REFERENCES

- 1 Siegel RL, Miller KD, Fuchs HE, Jemal A. Cancer statistics, 2022. *CA Cancer J Clin* 2022; **72**: 7-33 [PMID: 35020204 DOI: 10.3322/caac.21708]
- 2 Pu M, Messer K, Davies SR, Vickery TL, Pittman E, Parker BA, Ellis MJ, Flatt SW, Marinac CR, Nelson SH, Mardis ER, Pierce JP, Natarajan L. Research-based PAM50 signature and long-term breast cancer survival. *Breast Cancer Res Treat* 2020; **179**: 197-206 [PMID: 31542876 DOI: 10.1007/s10549-019-05446-y]
- 3 Tekpli X, Lien T, Røsevoid AH, Nebdal D, Borgen E, Ohnstad HO, Kyte JA, Vallon-Christersson J, Fongaard M, Due EU, Svartdal LG, Sveli MAT, Garred Ø, OSBREAC, Frigessi A, Sahlberg KK, Sørli T, Russnes HG, Naume B, Kristensen VN. An independent poor-prognosis subtype of breast cancer defined by a distinct tumor immune microenvironment. *Nat Commun* 2019; **10**: 5499 [PMID: 31796750 DOI: 10.1038/s41467-019-13329-5]
- 4 Wang M, Zhao J, Zhang L, Wei F, Lian Y, Wu Y, Gong Z, Zhang S, Zhou J, Cao K, Li X, Xiong W, Li G, Zeng Z, Guo C. Role of tumor microenvironment in tumorigenesis. *J Cancer* 2017; **8**: 761-773 [PMID: 28382138 DOI: 10.7150/jca.17648]
- 5 Dzobo K, Dandara C. Architecture of Cancer-Associated Fibroblasts in Tumor Microenvironment: Mapping Their Origins, Heterogeneity, and Role in Cancer Therapy Resistance. *OMICS* 2020; **24**: 314-339 [PMID: 32496970 DOI: 10.1089/omi.2020.0023]
- 6 Bertero T, Oldham WM, Grasset EM, Bourget I, Boulter E, Pisano S, Hofman P, Bellvert F, Meneguzzi G, Bulavin DV, Estrach S, Feral CC, Chan SY, Bozec A, Gaggioli C. Tumor-Stroma Mechanics Coordinate Amino Acid Availability to Sustain Tumor Growth and Malignancy. *Cell Metab* 2019; **29**: 124-140.e10 [PMID: 30293773 DOI: 10.1016/j.cmet.2018.09.012]
- 7 Gamradt P, De La Fouchardière C, Hennino A. Stromal Protein-Mediated Immune Regulation in Digestive Cancers. *Cancers (Basel)* 2021; **13** [PMID: 33466303 DOI: 10.3390/cancers13010146]
- 8 Kaur A, Ecker BL, Douglass SM, Kugel CH 3rd, Webster MR, Almeida FV, Somasundaram R, Hayden J, Ban E, Ahmadzadeh H, Franco-

- Barraza J, Shah N, Mellis IA, Keeney F, Kossenkov A, Tang HY, Yin X, Liu Q, Xu X, Fane M, Brafford P, Herlyn M, Speicher DW, Wargo JA, Tetzlaff MT, Haydu LE, Raj A, Shenoy V, Cukierman E, Weeraratna AT. Remodeling of the Collagen Matrix in Aging Skin Promotes Melanoma Metastasis and Affects Immune Cell Motility. *Cancer Discov* 2019; **9**: 64-81 [PMID: 30279173 DOI: 10.1158/2159-8290.CD-18-0193]
- 9 **Avalle L**, Raggi L, Monteleone E, Savino A, Viavattene D, Statello L, Camperi A, Stabile SA, Salemme V, De Marzo N, Marino F, Guglielmi C, Lobascio A, Zanini C, Forni M, Incarnato D, Defilippi P, Oliviero S, Poli V. STAT3 induces breast cancer growth via ANGPTL4, MMP13 and STC1 secretion by cancer associated fibroblasts. *Oncogene* 2022; **41**: 1456-1467 [PMID: 35042959 DOI: 10.1038/s41388-021-02172-y]
- 10 **Zeng H**, Hou Y, Zhou X, Lang L, Luo H, Sun Y, Wan X, Yuan T, Wang R, Liu Y, Tang R, Cheng S, Xu M, Liu M. Cancer-associated fibroblasts facilitate premetastatic niche formation through lncRNA SNHG5-mediated angiogenesis and vascular permeability in breast cancer. *Theranostics* 2022; **12**: 7351-7370 [PMID: 36438499 DOI: 10.7150/thno.74753]
- 11 **Fang WB**, Medrano M, Cote P, Portsche M, Rao V, Hong Y, Behbod F, Knapp JR, Bloomer C, Noel-Macdonnell J, Cheng N. Transcriptome analysis reveals differences in cell cycle, growth and migration related genes that distinguish fibroblasts derived from pre-invasive and invasive breast cancer. *Front Oncol* 2023; **13**: 1130911 [PMID: 37091166 DOI: 10.3389/fonc.2023.1130911]
- 12 **Langfelder P**, Horvath S. WGCNA: an R package for weighted correlation network analysis. *BMC Bioinformatics* 2008; **9**: 559 [PMID: 19114008 DOI: 10.1186/1471-2105-9-559]
- 13 **Zheng H**, Liu H, Li H, Dou W, Wang X. Weighted Gene Co-expression Network Analysis Identifies a Cancer-Associated Fibroblast Signature for Predicting Prognosis and Therapeutic Responses in Gastric Cancer. *Front Mol Biosci* 2021; **8**: 744677 [PMID: 34692770 DOI: 10.3389/fmolb.2021.744677]
- 14 **Liu B**, Chen X, Zhan Y, Wu B, Pan S. Identification of a Gene Signature for Renal Cell Carcinoma-Associated Fibroblasts Mediating Cancer Progression and Affecting Prognosis. *Front Cell Dev Biol* 2020; **8**: 604627 [PMID: 33634098 DOI: 10.3389/fcell.2020.604627]
- 15 **Harrow J**, Frankish A, Gonzalez JM, Tapanari E, Diekhans M, Kokocinski F, Aken BL, Barrell D, Zadissa A, Searle S, Barnes I, Bignell A, Boychenko V, Hunt T, Kay M, Mukherjee G, Rajan J, Despacio-Reyes G, Saunders G, Steward C, Harte R, Lin M, Howald C, Tanzer A, Derrien T, Chrast J, Walters N, Balasubramanian S, Pei B, Tress M, Rodriguez JM, Ezkurdia I, van Baren J, Brent M, Haussler D, Kellis M, Valencia A, Reymond A, Gerstein M, Guigó R, Hubbard TJ. GENCODE: the reference human genome annotation for The ENCODE Project. *Genome Res* 2012; **22**: 1760-1774 [PMID: 22955987 DOI: 10.1101/gr.135350.111]
- 16 **Wu SZ**, Al-Eryani G, Roden DL, Junankar S, Harvey K, Andersson A, Thennavan A, Wang C, Torpy JR, Bartonicek N, Wang T, Larsson L, Kaczorowski D, Weisenfeld NI, Uyttingco CR, Chew JG, Bent ZW, Chan CL, Gnanasambandapillai V, Dutertre CA, Gluch L, Hui MN, Beith J, Parker A, Robbins E, Segara D, Cooper C, Mak C, Chan B, Warrier S, Ginhoux F, Millar E, Powell JE, Williams SR, Liu XS, O'Toole S, Lim E, Lundeberg J, Perou CM, Swarbrick A. A single-cell and spatially resolved atlas of human breast cancers. *Nat Genet* 2021; **53**: 1334-1347 [PMID: 34493872 DOI: 10.1038/s41588-021-00911-1]
- 17 **Newman AM**, Liu CL, Green MR, Gentles AJ, Feng W, Xu Y, Hoang CD, Diehn M, Alizadeh AA. Robust enumeration of cell subsets from tissue expression profiles. *Nat Methods* 2015; **12**: 453-457 [PMID: 25822800 DOI: 10.1038/nmeth.3337]
- 18 **Yoshihara K**, Shahmoradgoli M, Martínez E, Vegesna R, Kim H, Torres-García W, Treviño V, Shen H, Laird PW, Levine DA, Carter SL, Getz G, Stenke-Hale K, Mills GB, Verhaak RG. Inferring tumour purity and stromal and immune cell admixture from expression data. *Nat Commun* 2013; **4**: 2612 [PMID: 24113773 DOI: 10.1038/ncomms3612]
- 19 **Yu G**, Wang LG, Han Y, He QY. clusterProfiler: an R package for comparing biological themes among gene clusters. *OMICS* 2012; **16**: 284-287 [PMID: 22455463 DOI: 10.1089/omi.2011.0118]
- 20 **Liberzon A**, Birger C, Thorvaldsdóttir H, Ghandi M, Mesirov JP, Tamayo P. The Molecular Signatures Database (MSigDB) hallmark gene set collection. *Cell Syst* 2015; **1**: 417-425 [PMID: 26771021 DOI: 10.1016/j.cels.2015.12.004]
- 21 **Hänzelmann S**, Castelo R, Guinney J. GSVA: gene set variation analysis for microarray and RNA-seq data. *BMC Bioinformatics* 2013; **14**: 7 [PMID: 23323831 DOI: 10.1186/1471-2105-14-7]
- 22 **Wang N**, Zhang H, Li D, Jiang C, Zhao H, Teng Y. Identification of novel biomarkers in breast cancer via integrated bioinformatics analysis and experimental validation. *Bioengineered* 2021; **12**: 12431-12446 [PMID: 34895070 DOI: 10.1080/21655979.2021.2005747]
- 23 **Wang X**, Li G, Zhang Y, Li L, Qiu L, Qian Z, Zhou S, Wang X, Li Q, Zhang H. Pan-Cancer Analysis Reveals Genomic and Clinical Characteristics of TRPV Channel-Related Genes. *Front Oncol* 2022; **12**: 813100 [PMID: 35174089 DOI: 10.3389/fonc.2022.813100]
- 24 **Kechagia JZ**, Ivaska J, Roca-Cusachs P. Integrins as biomechanical sensors of the microenvironment. *Nat Rev Mol Cell Biol* 2019; **20**: 457-473 [PMID: 31182865 DOI: 10.1038/s41580-019-0134-2]
- 25 **Mohammadi H**, Sahai E. Mechanisms and impact of altered tumour mechanics. *Nat Cell Biol* 2018; **20**: 766-774 [PMID: 29950570 DOI: 10.1038/s41556-018-0131-2]
- 26 **Shan T**, Chen S, Chen X, Lin WR, Li W, Ma J, Wu T, Ji H, Li Y, Cui X, Kang Y. Prometastatic mechanisms of CAF-mediated EMT regulation in pancreatic cancer cells. *Int J Oncol* 2017; **50**: 121-128 [PMID: 27878234 DOI: 10.3892/ijo.2016.3779]
- 27 **Herrera M**, Berral-González A, López-Cade I, Galindo-Pumariño C, Bueno-Fortes S, Martín-Merino M, Carrato A, Ocaña A, De La Pinta C, López-Alfonso A, Peña C, García-Barberán V, De Las Rivas J. Cancer-associated fibroblast-derived gene signatures determine prognosis in colon cancer patients. *Mol Cancer* 2021; **20**: 73 [PMID: 33926453 DOI: 10.1186/s12943-021-01367-x]
- 28 **Zhang Z**, Liang Z, Li D, Wang L, Chen Y, Liang Y, Jiao W, Niu H. Development of a CAFs-related gene signature to predict survival and drug response in bladder cancer. *Hum Cell* 2022; **35**: 649-664 [PMID: 35044630 DOI: 10.1007/s13577-022-00673-w]
- 29 **Monteran L**, Erez N. The Dark Side of Fibroblasts: Cancer-Associated Fibroblasts as Mediators of Immunosuppression in the Tumor Microenvironment. *Front Immunol* 2019; **10**: 1835 [PMID: 31428105 DOI: 10.3389/fimmu.2019.01835]
- 30 **Wu X**, Zhou Z, Xu S, Liao C, Chen X, Li B, Peng J, Li D, Yang L. Extracellular vesicle packaged LMP1-activated fibroblasts promote tumor progression via autophagy and stroma-tumor metabolism coupling. *Cancer Lett* 2020; **478**: 93-106 [PMID: 32160975 DOI: 10.1016/j.canlet.2020.03.004]
- 31 **Puram SV**, Tirosh I, Parkih AS, Patel AP, Yizhak K, Gillespie S, Rodman C, Luo CL, Mroz EA, Emerick KS, Deschler DG, Varvares MA, Mylvaganam R, Rozenblatt-Rosen O, Rocco JW, Faquin WC, Lin DT, Regev A, Bernstein BE. Single-Cell Transcriptomic Analysis of Primary and Metastatic Tumor Ecosystems in Head and Neck Cancer. *Cell* 2017; **171**: 1611-1624.e24 [PMID: 29198524 DOI: 10.1016/j.cell.2017.10.044]
- 32 **Qian J**, Olbrecht S, Boeckx B, Vos H, Laoui D, Etioglu E, Wauters E, Pomella V, Verbandt S, Busschaert P, Bassez A, Franken A, Bempt MV, Xiong J, Weynand B, van Herck Y, Antoranz A, Bosisio FM, Thienpont B, Floris G, Vergote I, Smeets A, Tejpar S, Lambrechts D. A pan-cancer blueprint of the heterogeneous tumor microenvironment revealed by single-cell profiling. *Cell Res* 2020; **30**: 745-762 [PMID: 32561858 DOI: 10.1038/s41422-020-0355-0]

- 33 **Öhlund D**, Handly-Santana A, Biffi G, Elyada E, Almeida AS, Ponz-Sarvise M, Corbo V, Oni TE, Hearn SA, Lee EJ, Chio II, Hwang CI, Tiriac H, Baker LA, Engle DD, Feig C, Kultti A, Egeblad M, Fearon DT, Crawford JM, Clevers H, Park Y, Tuveson DA. Distinct populations of inflammatory fibroblasts and myofibroblasts in pancreatic cancer. *J Exp Med* 2017; **214**: 579-596 [PMID: 28232471 DOI: 10.1084/jem.20162024]
- 34 **Elyada E**, Bolisetty M, Laise P, Flynn WF, Courtois ET, Burkhart RA, Teinor JA, Belleau P, Biffi G, Lucito MS, Sivajothi S, Armstrong TD, Engle DD, Yu KH, Hao Y, Wolfgang CL, Park Y, Preall J, Jaffee EM, Califano A, Robson P, Tuveson DA. Cross-Species Single-Cell Analysis of Pancreatic Ductal Adenocarcinoma Reveals Antigen-Presenting Cancer-Associated Fibroblasts. *Cancer Discov* 2019; **9**: 1102-1123 [PMID: 31197017 DOI: 10.1158/2159-8290.CD-19-0094]
- 35 **Biffi G**, Oni TE, Spielman B, Hao Y, Elyada E, Park Y, Preall J, Tuveson DA. IL1-Induced JAK/STAT Signaling Is Antagonized by TGF β to Shape CAF Heterogeneity in Pancreatic Ductal Adenocarcinoma. *Cancer Discov* 2019; **9**: 282-301 [PMID: 30366930 DOI: 10.1158/2159-8290.CD-18-0710]
- 36 **Wang Y**, Lv W, Yi Y, Zhang Q, Zhang J, Wu Y. A novel signature based on cancer-associated fibroblast genes to predict prognosis, immune feature, and therapeutic response in breast cancer. *Aging (Albany NY)* 2023; **15**: 3480-3497 [PMID: 37142271 DOI: 10.18632/aging.204685]
- 37 **Huang B**, Chen Q, Ye Z, Zeng L, Huang C, Xie Y, Zhang R, Shen H. Construction of a Matrix Cancer-Associated Fibroblast Signature Gene-Based Risk Prognostic Signature for Directing Immunotherapy in Patients with Breast Cancer Using Single-Cell Analysis and Machine Learning. *Int J Mol Sci* 2023; **24** [PMID: 37685980 DOI: 10.3390/ijms241713175]
- 38 **Xu A**, Xu XN, Luo Z, Huang X, Gong RQ, Fu DY. Identification of prognostic cancer-associated fibroblast markers in luminal breast cancer using weighted gene co-expression network analysis. *Front Oncol* 2023; **13**: 1191660 [PMID: 37207166 DOI: 10.3389/fonc.2023.1191660]
- 39 **Li Z**, Yu X, Werner J, Bazhin AV, D'Haese JG. The role of interleukin-18 in pancreatitis and pancreatic cancer. *Cytokine Growth Factor Rev* 2019; **50**: 1-12 [PMID: 31753718 DOI: 10.1016/j.cytogfr.2019.11.001]
- 40 **Ma T**, Kong M. Interleukin-18 and -10 may be associated with lymph node metastasis in breast cancer. *Oncol Lett* 2021; **21**: 253 [PMID: 33664817 DOI: 10.3892/ol.2021.12515]
- 41 **Szekely B**, Bossuyt V, Li X, Wali VB, Patwardhan GA, Frederick C, Silber A, Park T, Harigopal M, Pelekanou V, Zhang M, Yan Q, Rimm DL, Bianchini G, Hatzis C, Pusztai L. Immunological differences between primary and metastatic breast cancer. *Ann Oncol* 2018; **29**: 2232-2239 [PMID: 30203045 DOI: 10.1093/annonc/mdy399]
- 42 **Rasmussen LM**, Frederiksen KS, Din N, Galsgaard E, Christensen L, Berchtold MW, Panina S. Prolactin and oestrogen synergistically regulate gene expression and proliferation of breast cancer cells. *Endocr Relat Cancer* 2010; **17**: 809-822 [PMID: 20601496 DOI: 10.1677/ERC-09-0326]
- 43 **Degen M**, Brellier F, Kain R, Ruiz C, Terracciano L, Orend G, Chiquet-Ehrismann R. Tenascin-W is a novel marker for activated tumor stroma in low-grade human breast cancer and influences cell behavior. *Cancer Res* 2007; **67**: 9169-9179 [PMID: 17909022 DOI: 10.1158/0008-5472.CAN-07-0666]
- 44 **Montagner M**, Enzo E, Forcato M, Zanconato F, Parenti A, Rampazzo E, Basso G, Leo G, Rosato A, Biciato S, Cordenonsi M, Piccolo S. SHARP1 suppresses breast cancer metastasis by promoting degradation of hypoxia-inducible factors. *Nature* 2012; **487**: 380-384 [PMID: 22801492 DOI: 10.1038/nature11207]
- 45 **Lampis A**, Carotenuto P, Vlachogiannis G, Cascione L, Hedayat S, Burke R, Clarke P, Bosma E, Simbolo M, Scarpa A, Yu S, Cole R, Smyth E, Mateos JF, Begum R, Hezelova B, Eltahir Z, Wotherspoon A, Fotiadis N, Bali MA, Nepal C, Khan K, Stubbs M, Hahne JC, Gasparini P, Guzzardo V, Croce CM, Eccles S, Fassan M, Cunningham D, Andersen JB, Workman P, Valeri N, Braconi C. MIR21 Drives Resistance to Heat Shock Protein 90 Inhibition in Cholangiocarcinoma. *Gastroenterology* 2018; **154**: 1066-1079.e5 [PMID: 29113809 DOI: 10.1053/j.gastro.2017.10.043]
- 46 **Ghoorun RA**, Wu XH, Chen HL, Ren DL, Wu XB. Prognostic Significance of FKBP14 in Gastric Cancer. *Onco Targets Ther* 2019; **12**: 11567-11577 [PMID: 31920344 DOI: 10.2147/OTT.S221943]
- 47 **Lu M**, Miao Y, Qi L, Bai M, Zhang J, Feng Y. RNAi-Mediated Downregulation of FKBP14 Suppresses the Growth of Human Ovarian Cancer Cells. *Oncol Res* 2016; **23**: 267-274 [PMID: 27131312 DOI: 10.3727/096504016X14549667333963]



Published by **Baishideng Publishing Group Inc**
7041 Koll Center Parkway, Suite 160, Pleasanton, CA 94566, USA
Telephone: +1-925-3991568
E-mail: office@baishideng.com
Help Desk: <https://www.f6publishing.com/helpdesk>
<https://www.wjgnet.com>

